US011119042B2

(12) **United States Patent**
Dutta et al.

(10) **Patent No.: US 11,119,042 B2**
(45) **Date of Patent: Sep. 14, 2021**

(54) **ALL-OPTICAL WRITE/READ SCHEME FOR MAGNETIC NANOSTRUCTURES**

(71) Applicant: **Purdue Research Foundation**, West Lafayette, IN (US)

(72) Inventors: **Aveek Dutta**, West Lafayette, IN (US); **Vladimir M. Shalaev**, West Lafayette, IN (US); **Alexandra Boltasseva**, West Lafayette, IN (US); **Esteban E. Marinero-Caceres**, West Lafayette, IN (US)

(73) Assignee: **Purdue Research Foundation**, West Lafayette, IN (US)

(*) Notice: Subject to any disclaimer, the term of this patent is extended or adjusted under 35 U.S.C. 154(b) by 0 days.

(21) Appl. No.: **16/990,754**

(22) Filed: **Aug. 11, 2020**

(65) **Prior Publication Data**

US 2020/0371026 A1 Nov. 26, 2020

Related U.S. Application Data

(63) Continuation of application No. 16/399,917, filed on Apr. 30, 2019, now Pat. No. 10,739,261.
(Continued)

(51) **Int. Cl.**
G01N 21/552 (2014.01)
G01N 21/01 (2006.01)
(Continued)

(52) **U.S. Cl.**
CPC ***G01N 21/553*** (2013.01); ***G01N 21/01*** (2013.01); ***G01R 33/1215*** (2013.01); *B82Y 20/00* (2013.01);
(Continued)

(58) **Field of Classification Search**
CPC G01N 2021/0162; G01N 21/553; G01N 21/01; B82Y 20/00; B82Y 35/00;
(Continued)

(56) **References Cited**

U.S. PATENT DOCUMENTS

7,760,053 B2 * 7/2010 Kochergin G02B 1/007 333/208
9,105,832 B2 * 8/2015 Buhrman G11C 11/1673
(Continued)

Primary Examiner — Hoa Q Pham
(74) *Attorney, Agent, or Firm* — Piroozi-IP, LLC

(57) **ABSTRACT**

A system of writing to and reading from a magnetic nanostructure is disclosed which includes an opto-magnetic write arrangement including a polarizer configured to receive incident light and provide a circularly or linearly polarized light, wherein light polarization is controlled by the polarizer and its orientation with respect to polarization of the incident light, a nanomagnetic structure configured to receive the polarized light including a substrate, and a nanomagnetic stack including a nanomagnet, and a capping layer, wherein the nanomagnetic stack is configured to receive the polarized light and thereby switch orientation of a magnetic moment associated with the magnetic nanostructure whereby the magnetic moment direction specifies a bit value held in the magnetic structure, and a magnetic read arrangement, configured to receive and interpret an optical signal from the magnetic nanostructure indicating the magnetic moment orientation from the nanomagnetic stack.

8 Claims, 18 Drawing Sheets

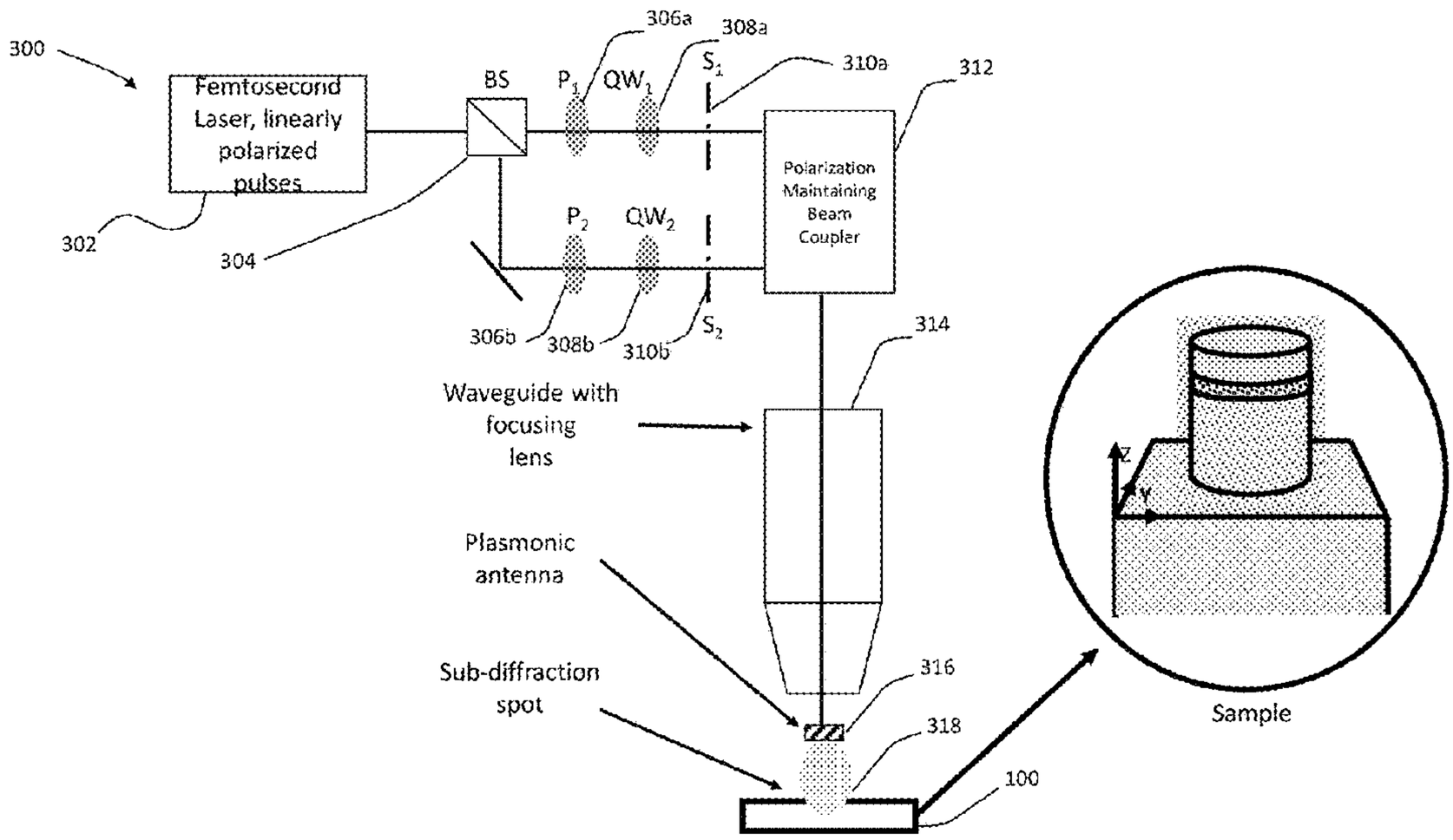

Related U.S. Application Data

(60) Provisional application No. 62/664,925, filed on Apr. 30, 2018.

(51) **Int. Cl.**

G01R 33/12	(2006.01)
B82Y 20/00	(2011.01)
B82Y 35/00	(2011.01)

(52) **U.S. Cl.**
CPC *B82Y 35/00* (2013.01); *G01N 2021/0162* (2013.01)

(58) **Field of Classification Search**
CPC ... G01R 33/1215; H01F 10/123; H01L 43/08; H01L 43/10; H01L 43/12; H01L 27/222
USPC 356/445–448, 364–369
See application file for complete search history.

(56) **References Cited**

U.S. PATENT DOCUMENTS

10,739,261	B2 *	8/2020	Dutta	G01N 21/01
2012/0280336	A1 *	11/2012	Jan	H01L 43/12 257/421
2013/0121068	A1 *	5/2013	Ruotolo	G11C 11/1693 365/158
2015/0177239	A1 *	6/2015	Evers	G01N 33/54366 435/6.1
2017/0279038	A1 *	9/2017	Wu	H01L 43/10
2018/0003865	A1 *	1/2018	Guler	B01J 27/24
2019/0353830	A1 *	11/2019	Kildishev	G11B 7/1381
2020/0048084	A1 *	2/2020	Acosta	G01R 33/12
2021/0103011	A1 *	4/2021	Noh	H01L 43/12

* cited by examiner

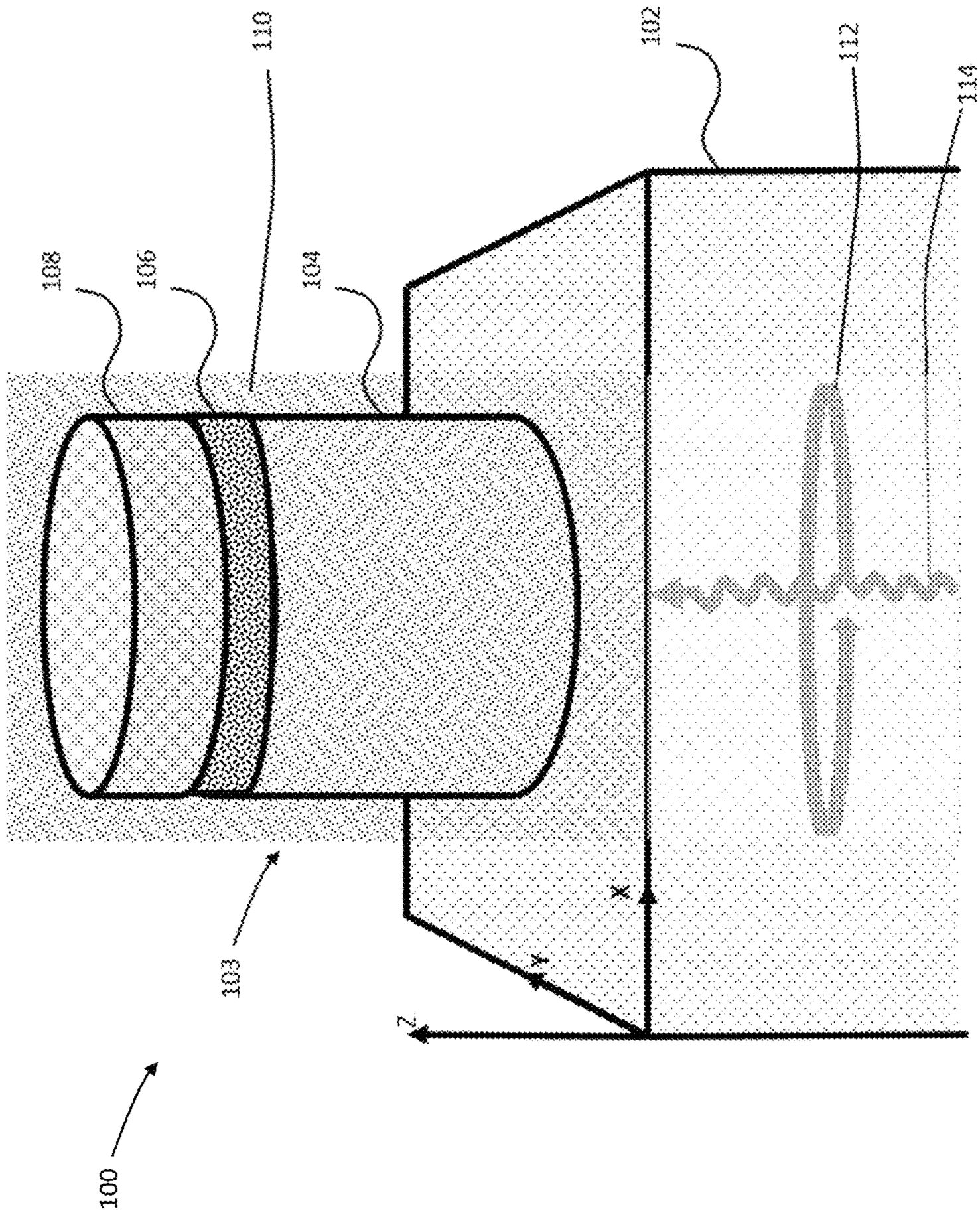

FIG. 1

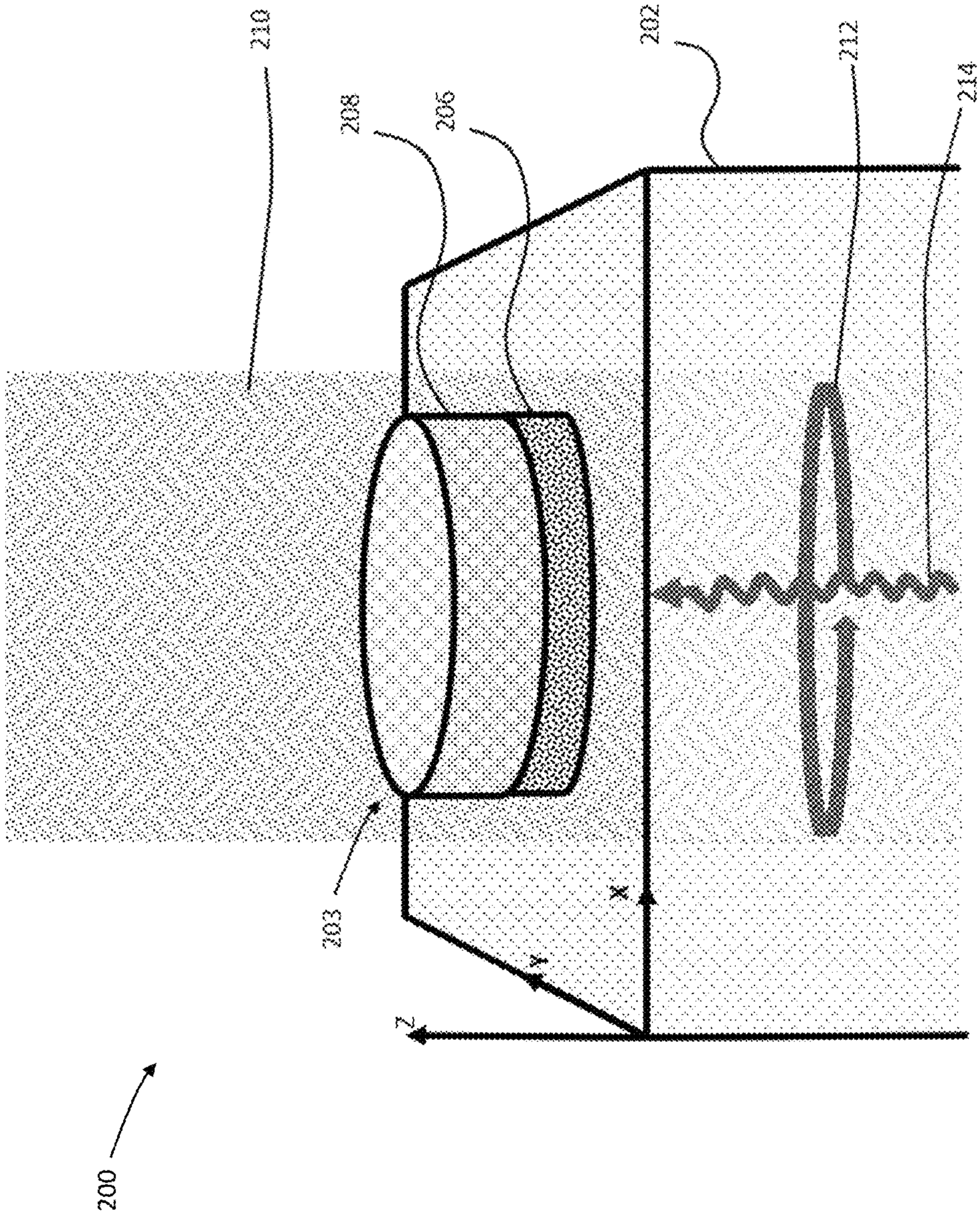

FIG. 2

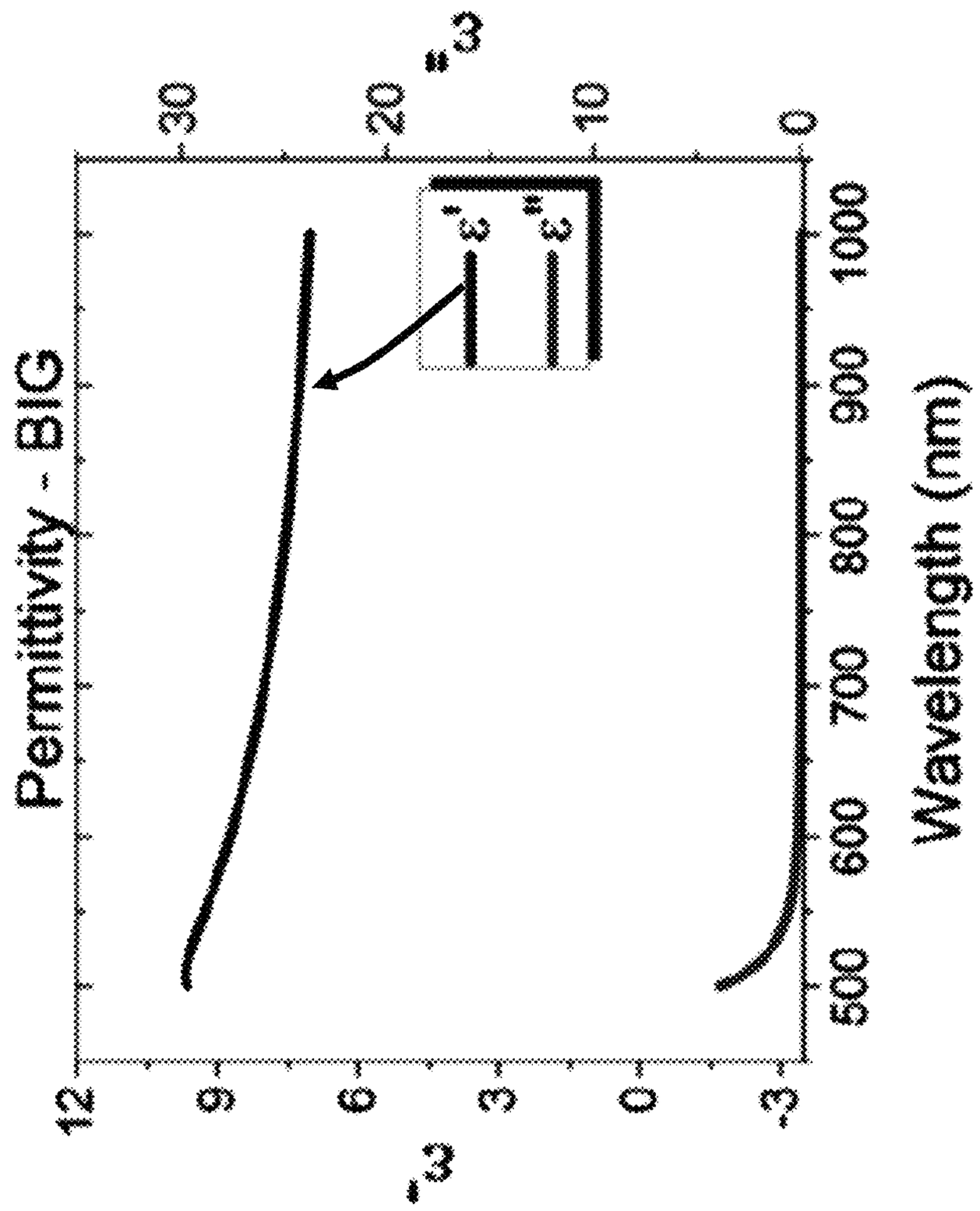

FIG. 3

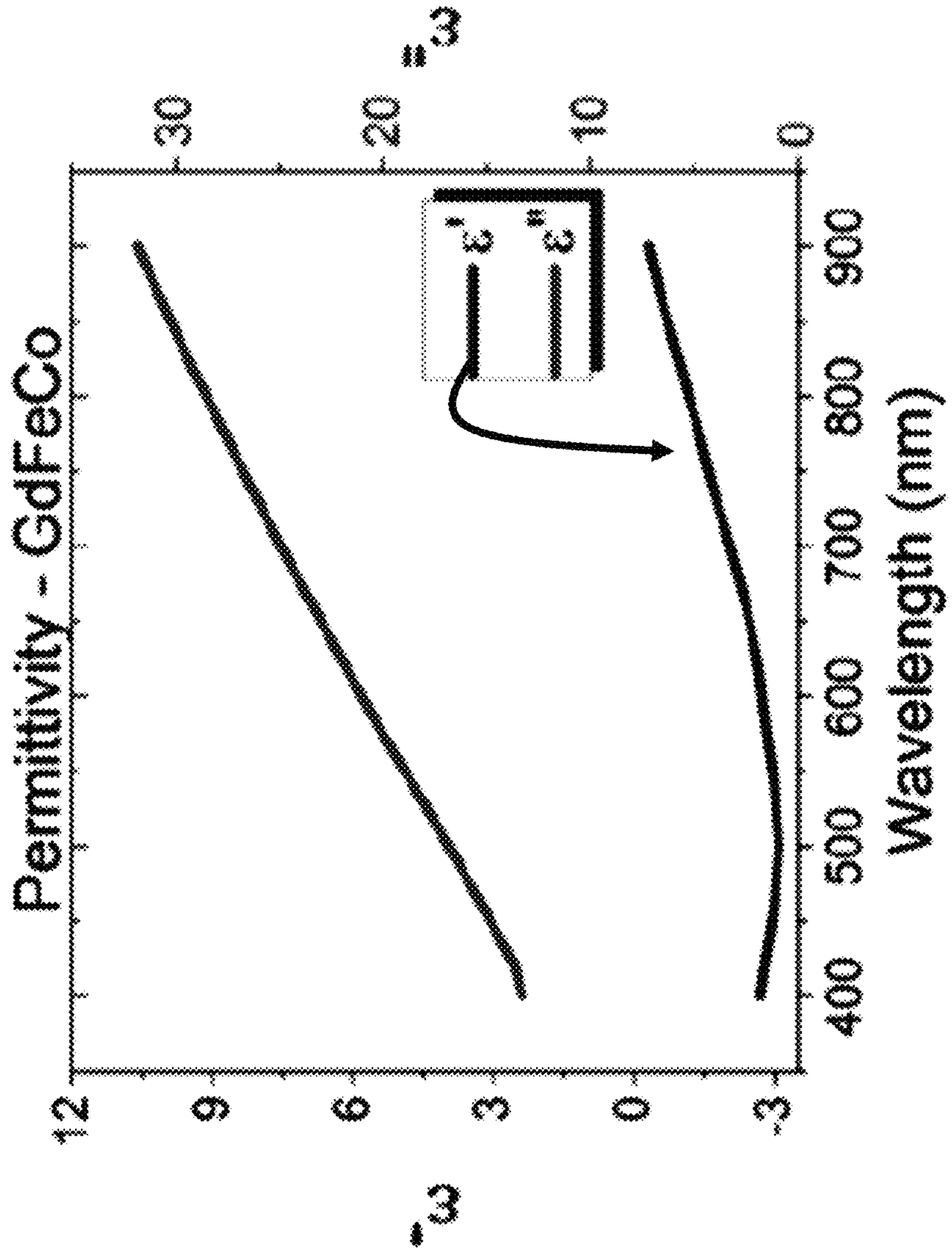
Permittivity - GdFeCo
Wavelength (nm)
400
500
600
700
800
900
-40
-30
-20
-10
0
10
20
30
ε'
ε''

FIG. 4

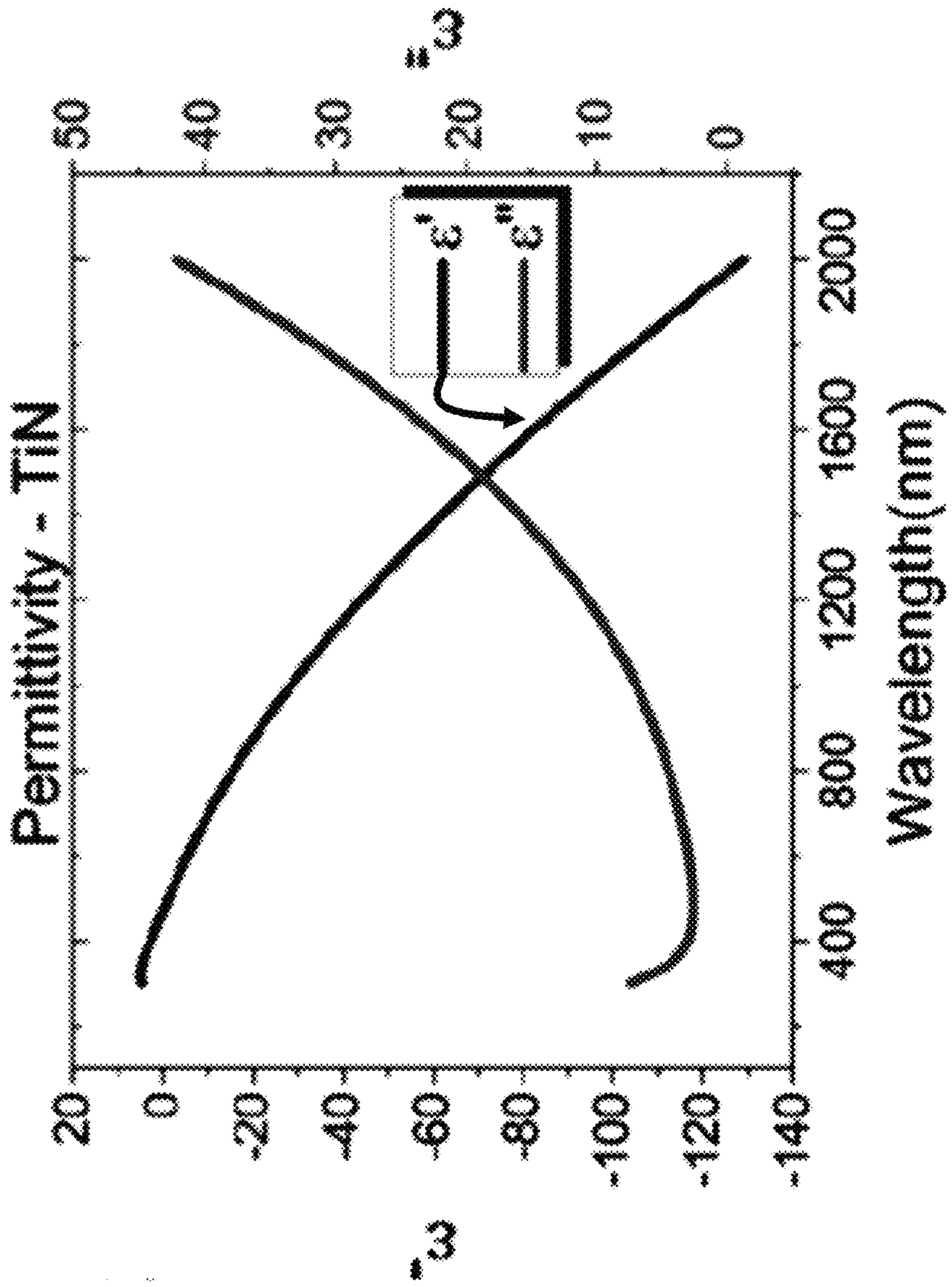
Permittivity - TiN
Wavelength(nm)
400
800
1200
1600
2000
60
40
30
20
10
0
-20
-40
-60
-80
-100
-120
-140
ε''
ε'
ε''
ε'

FIG. 5

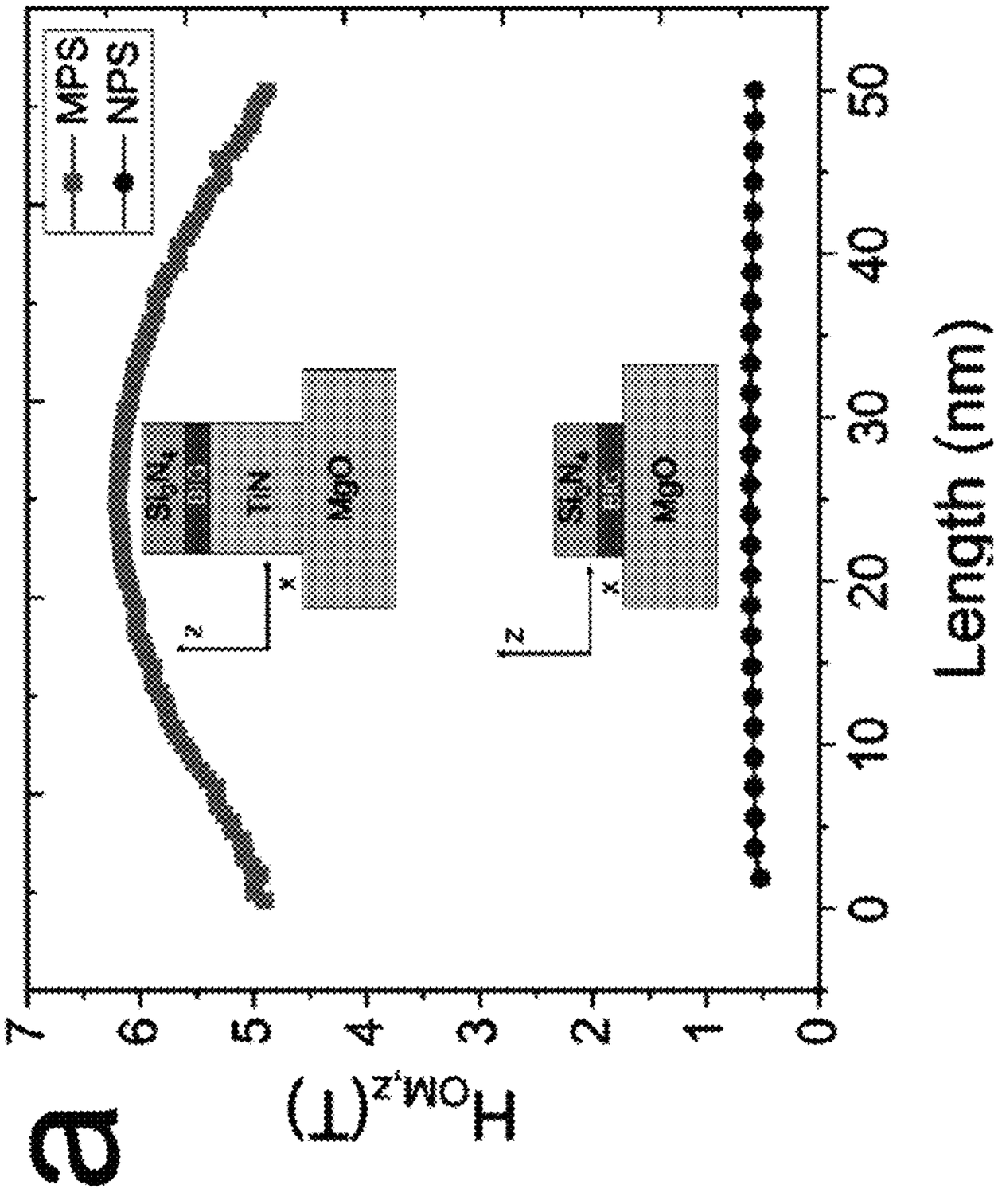
MPS
NPS
Si_3N_4
ITO
TiN
MgO
z
x
Si_3N_4
ITO
MgO
z
x
0
10
20
30
40
50
Length (nm)
0
1
2
3
4
5
6
7
$H_{OM,z}(T)$

FIG. 6a

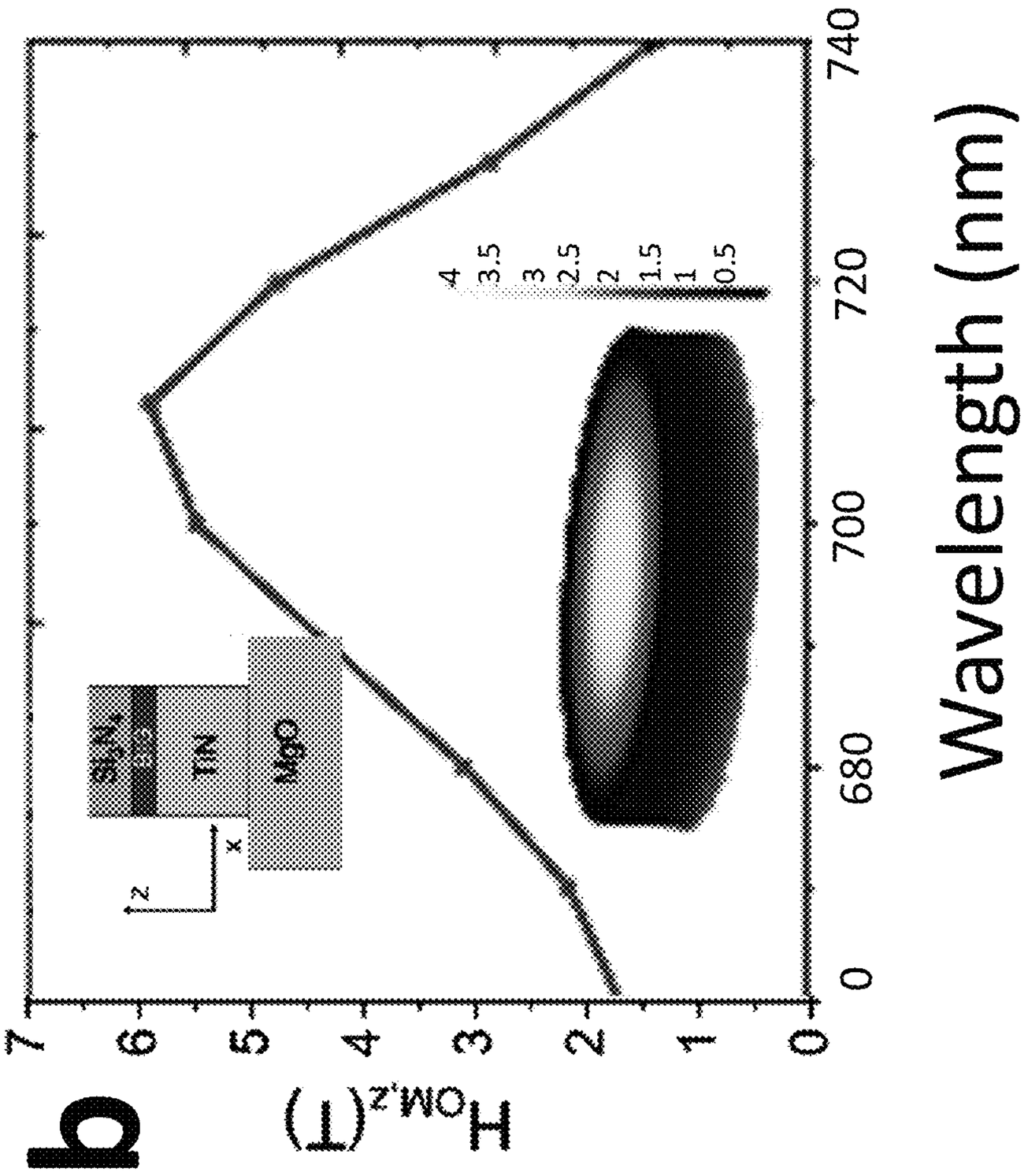
Si3N4
TiN
MgO
z
x
4
3.5
3
2.5
2
1.5
1
0.5
0
680
700
720
740
Wavelength (nm)
$H_{OM,z}(T)$
0
1
2
3
4
5
6
7

FIG. 6b

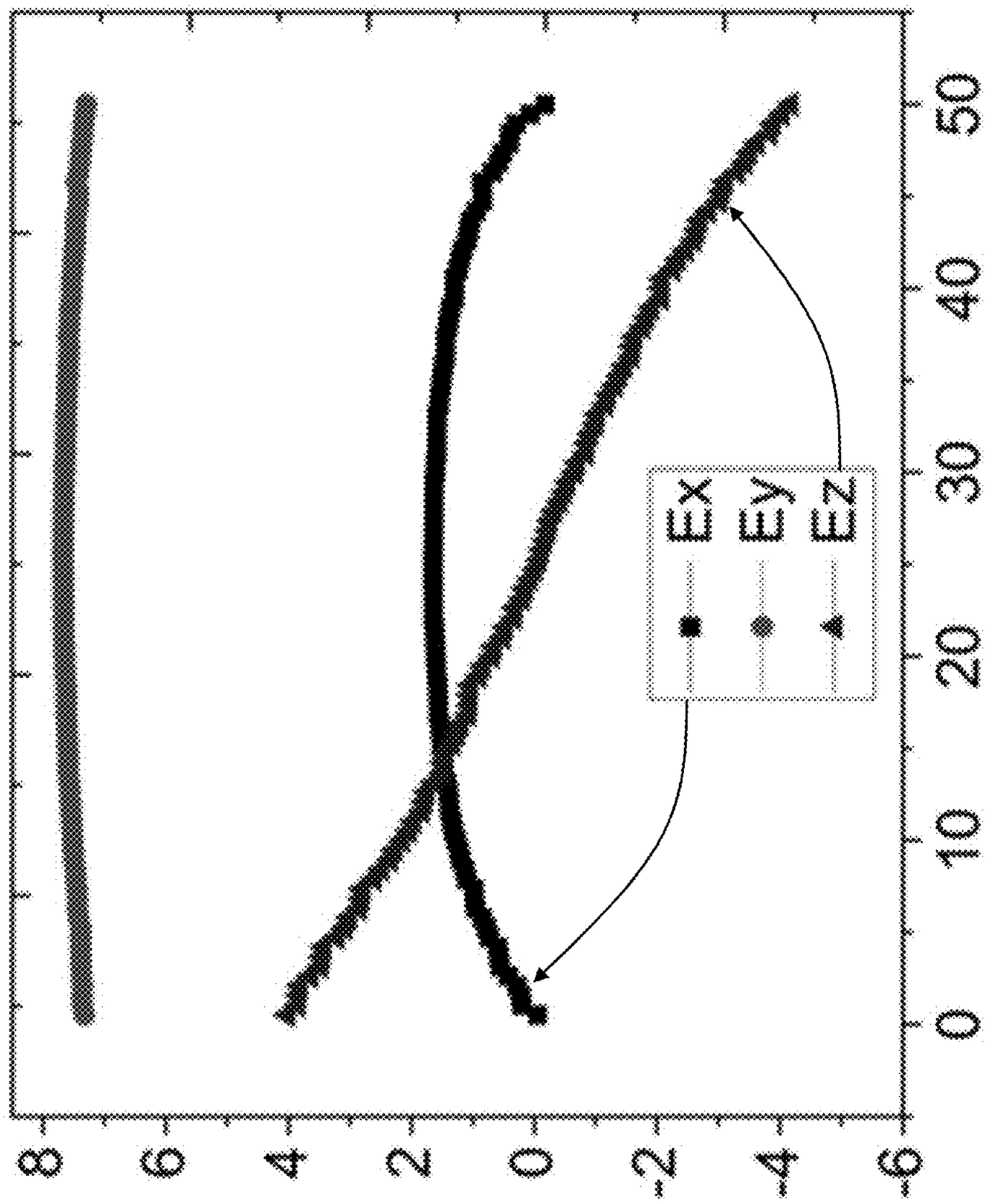

FIG. 7a

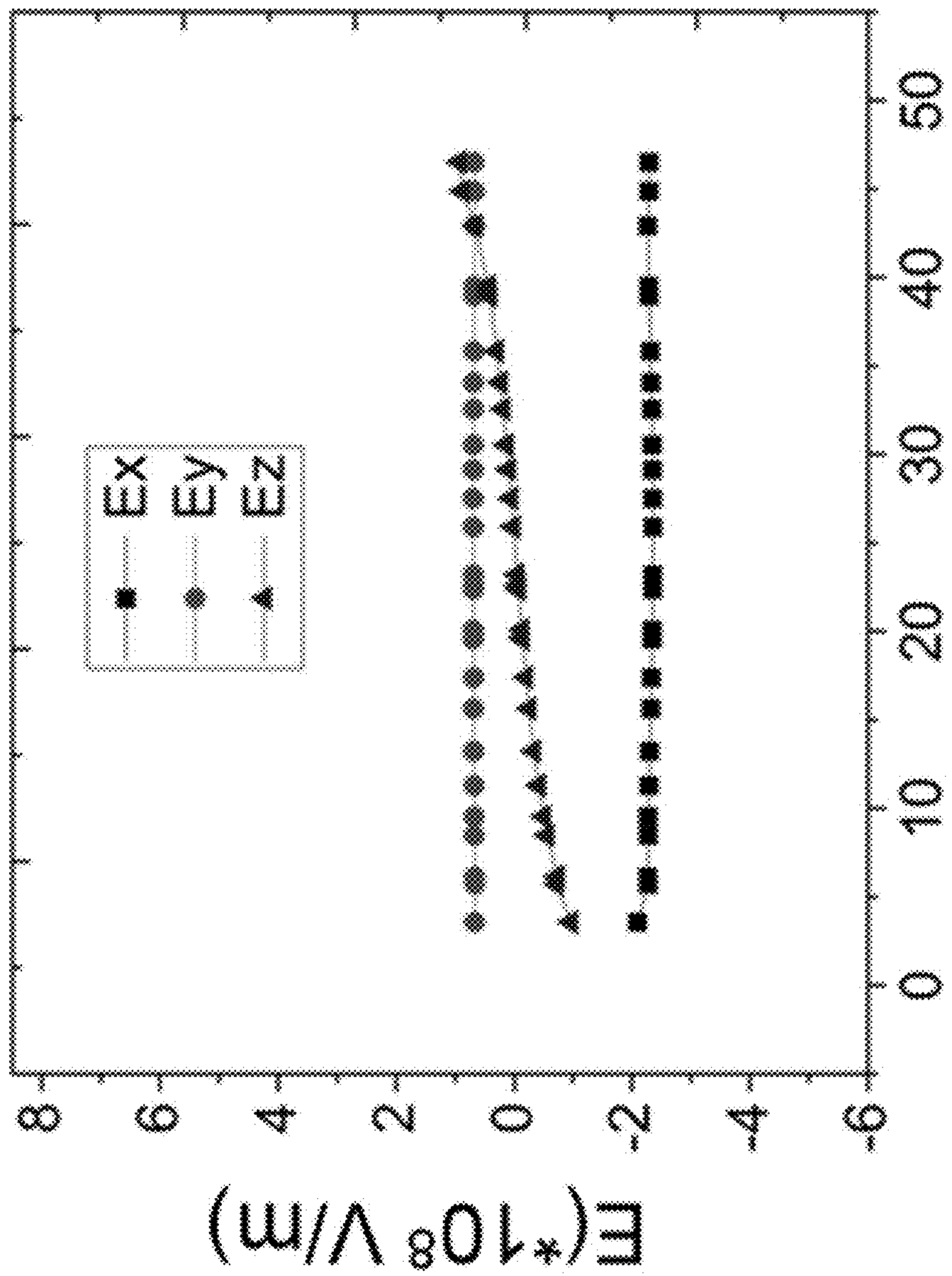

FIG. 7c

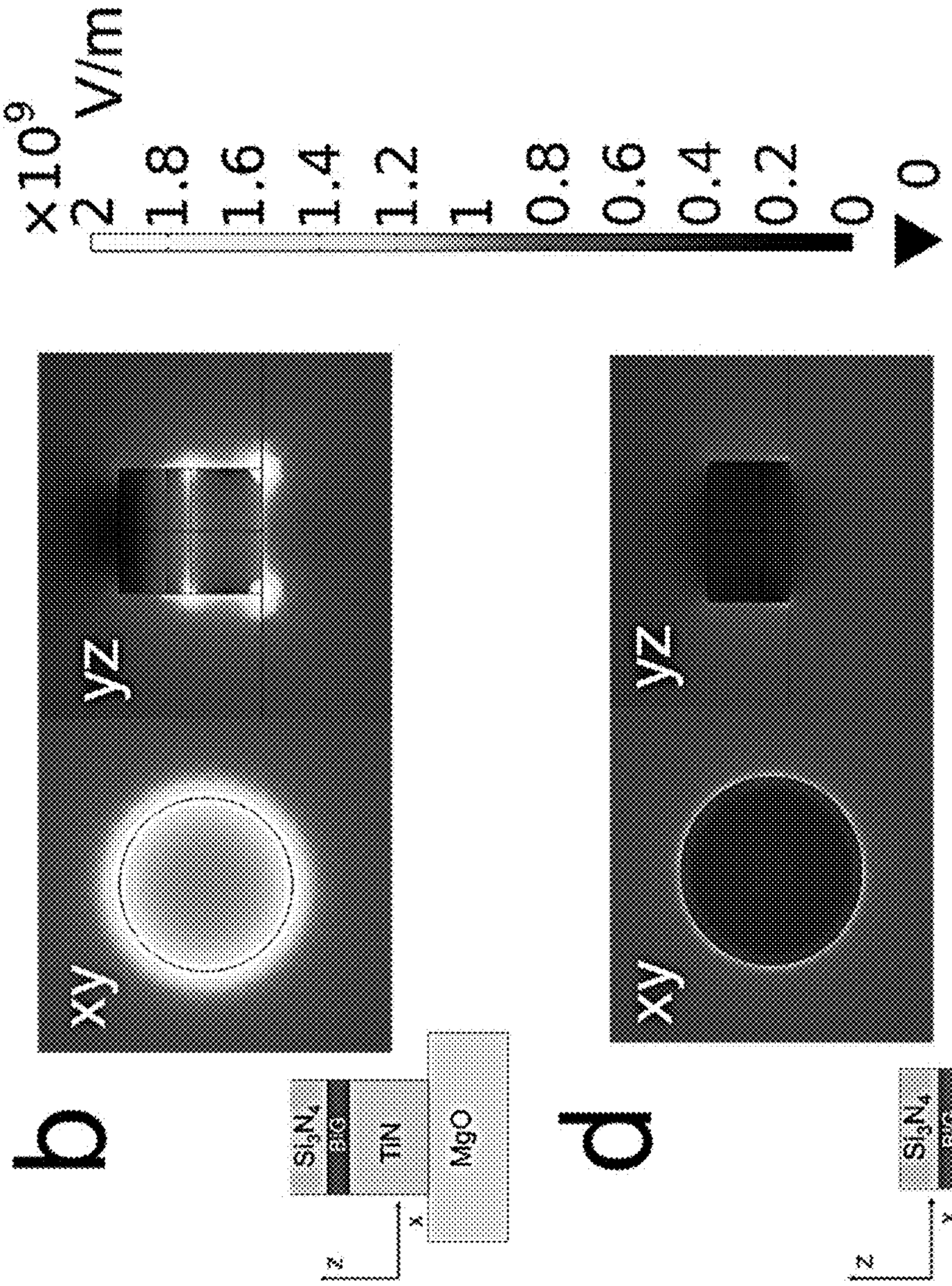

FIGs. 7b and 7d

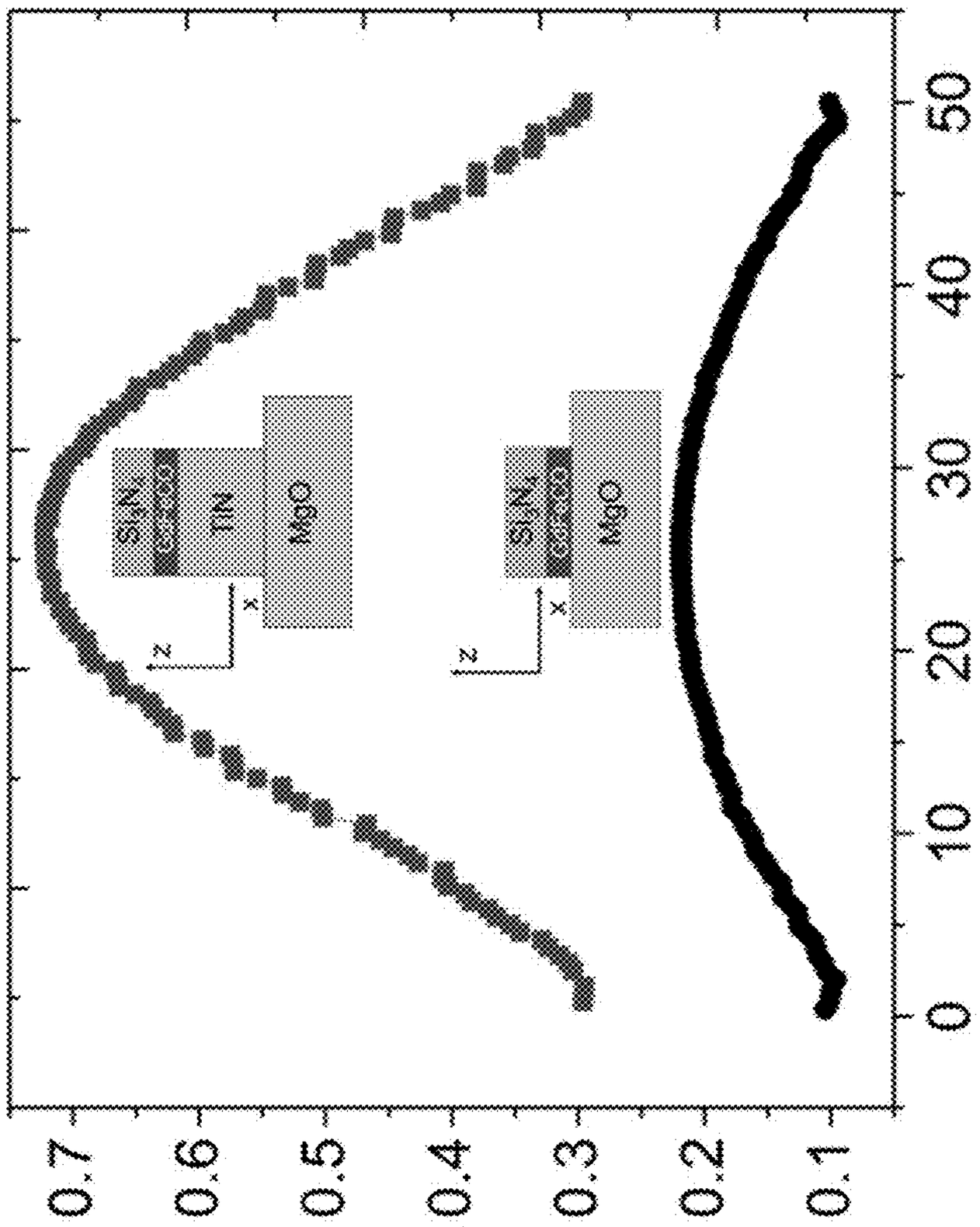
a
$H_{OM,z}$ (T)
0.7
0.6
0.5
0.4
0.3
0.2
0.1
Length (nm)
0
10
20
30
40
50
Si3N4
Ta
TiN
MgO
z
x

FIG. 8a

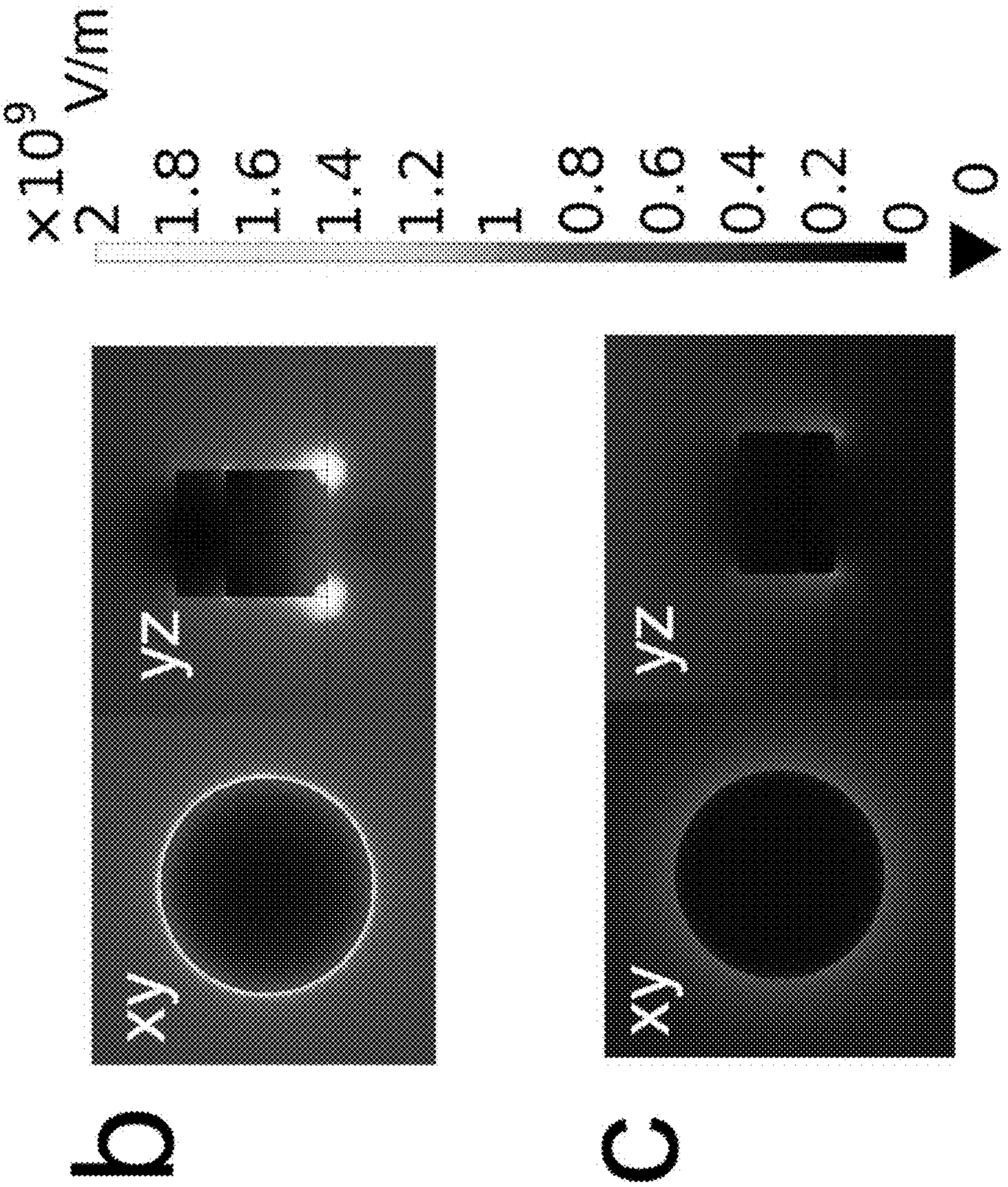

FIGs. 8b and 8c

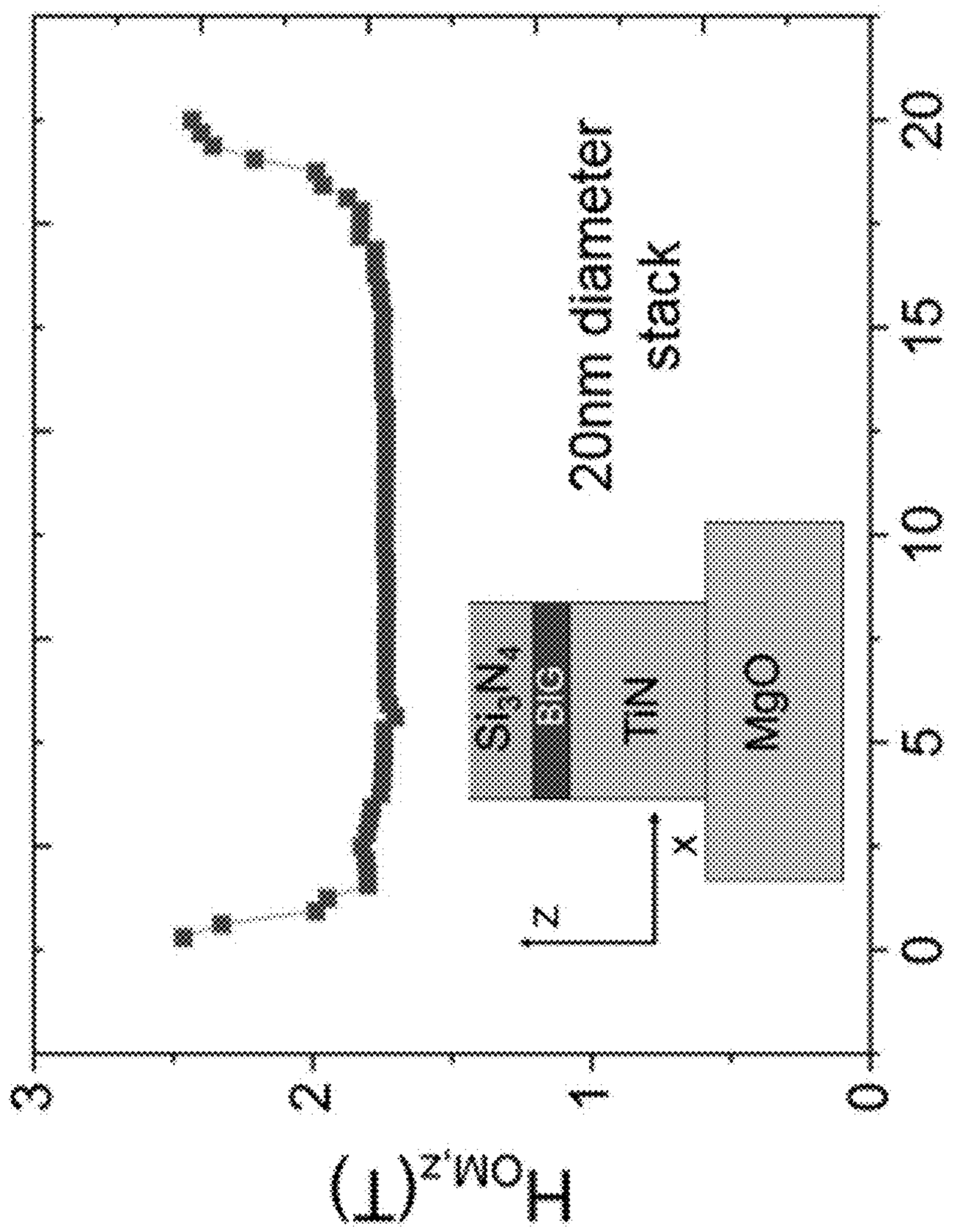
$H_{OM,z}$ (T)
3
2
1
0
z
x
Si_3N_4
BIG
TiN
MgO
20nm diameter
stack
0
5
10
15
20
Length (nm)

FIG. 9

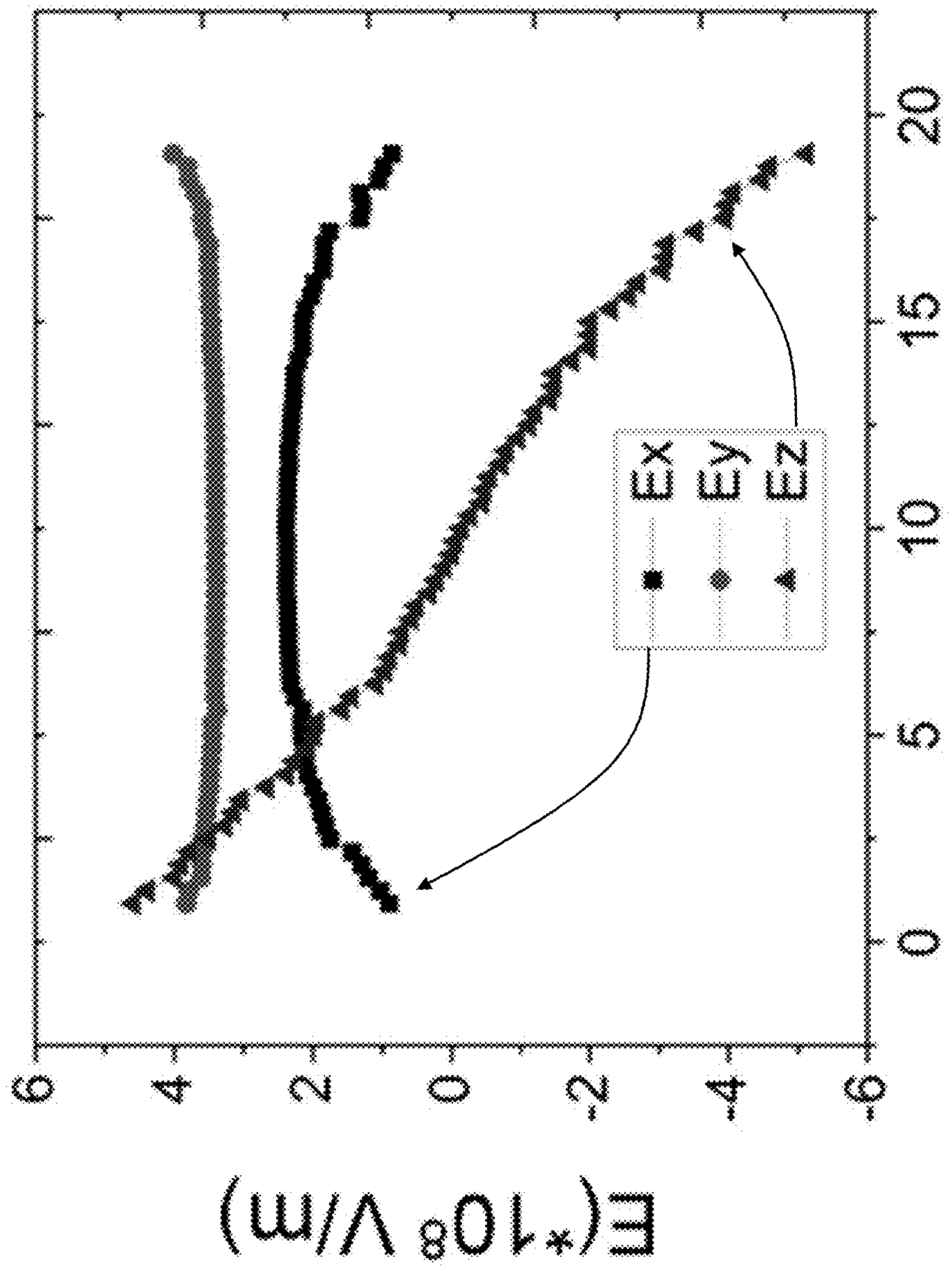

FIG. 10

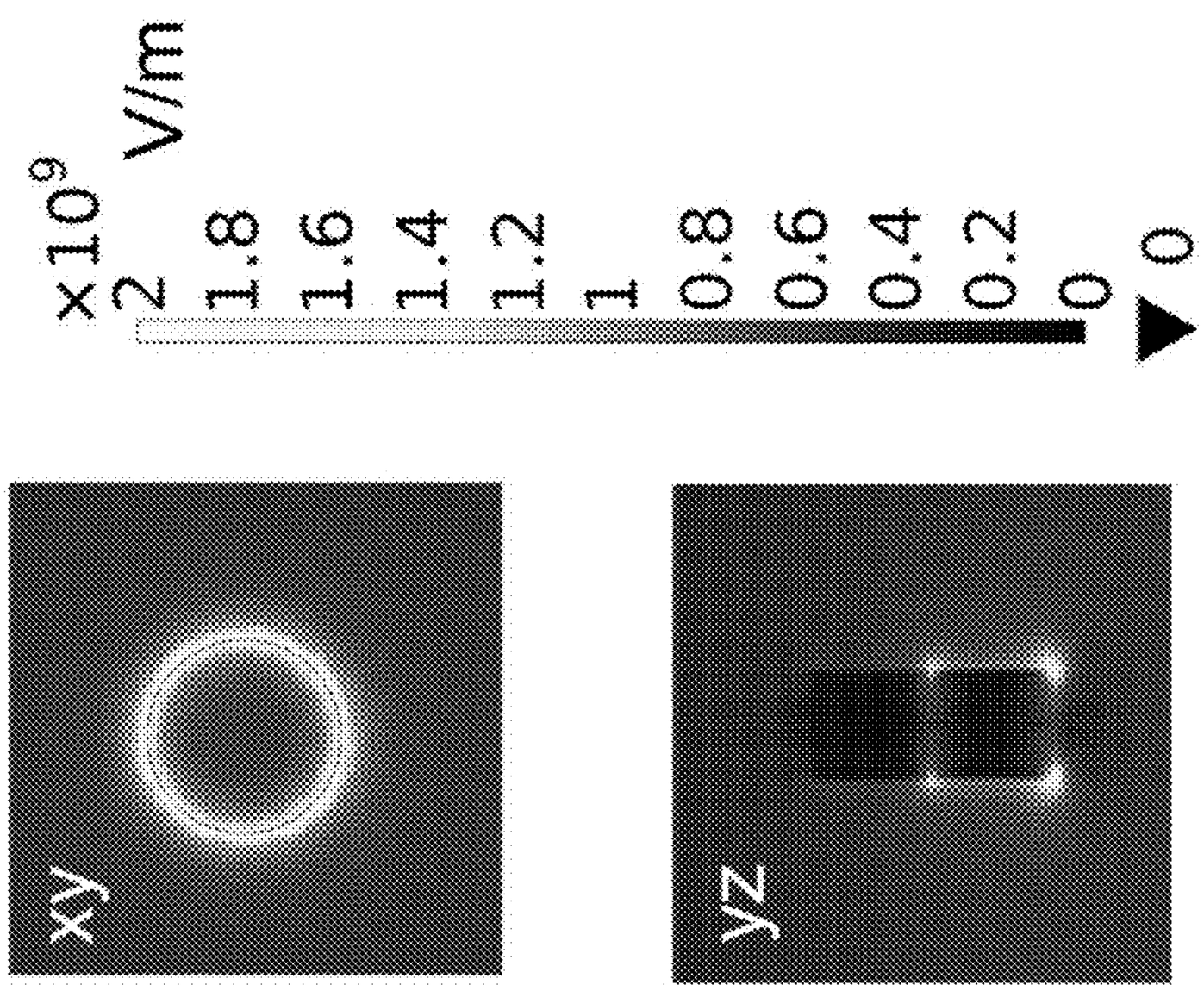

FIGs. 11a and 11b

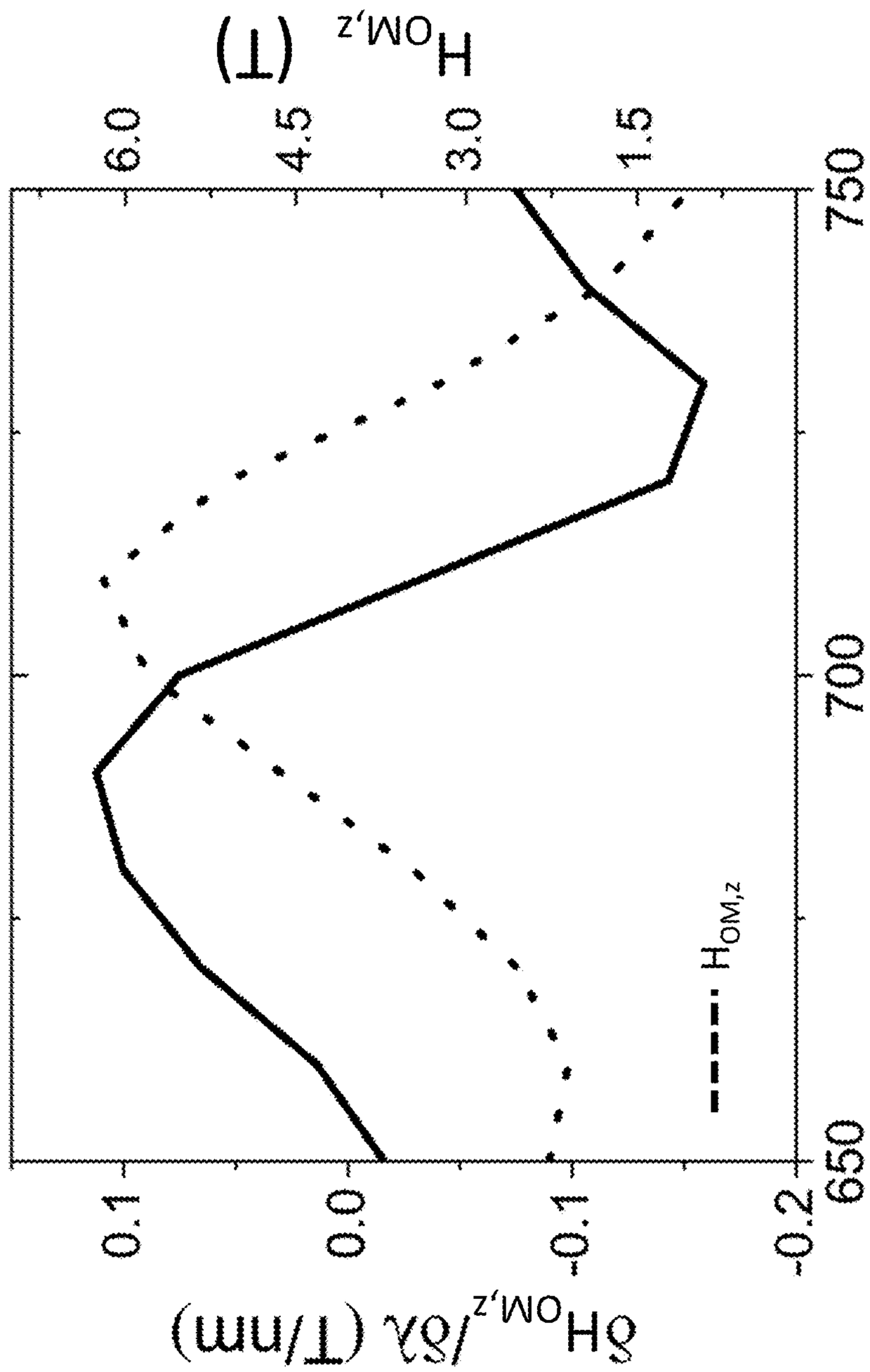
$H_{OM,z}$ (T)
6.0
4.5
3.0
1.5
0
750
700
650
Wavelength (nm)
$H_{OM,z}$
0.1
0.0
-0.1
-0.2
$\delta H_{OM,z}/\delta\lambda$ (T/nm)

FIG. 12

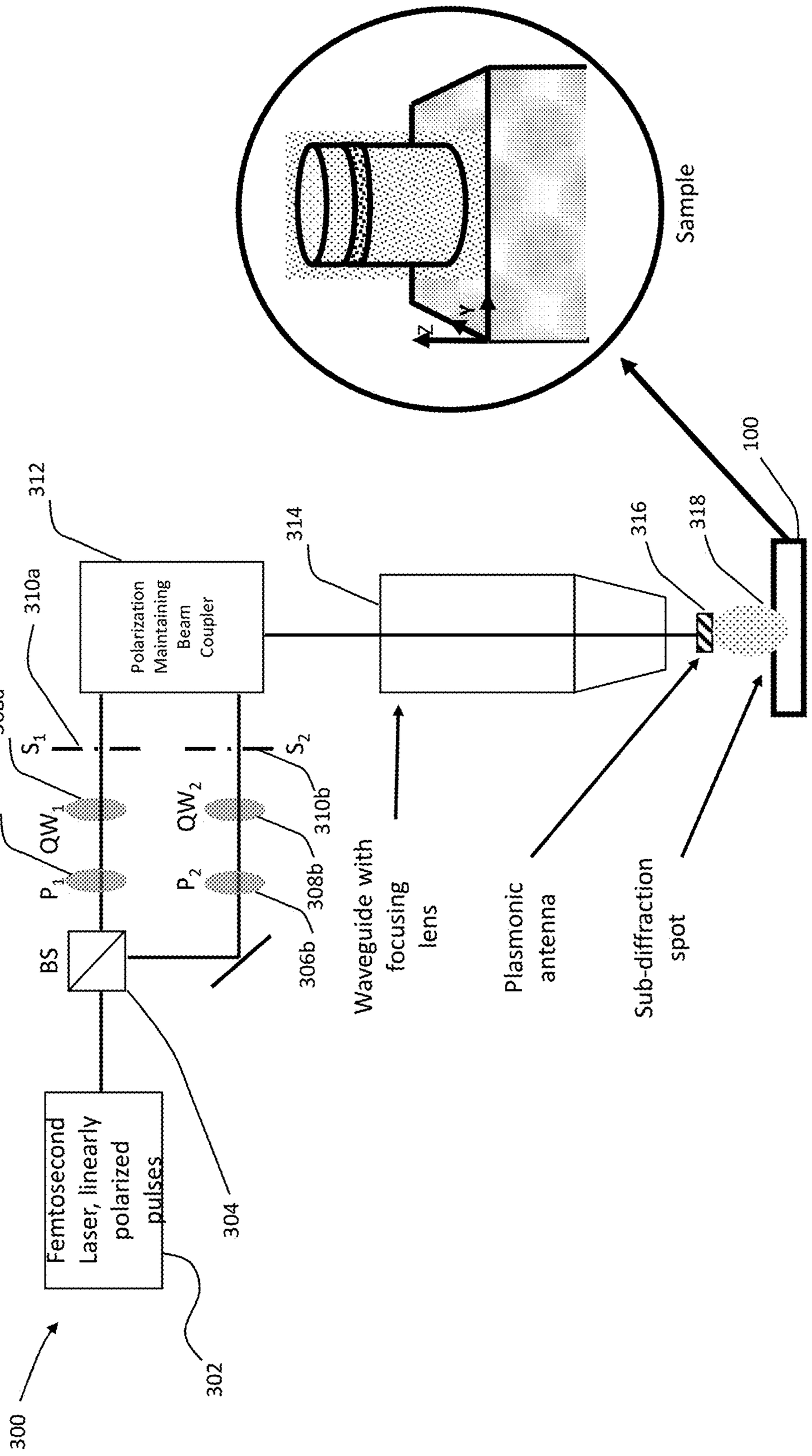
Sample
Z
Y
100
312
Polarization Maintaining Beam Coupler
310a
314
316
318
308a
306a
S_1
QW_1
P_1
P_2
QW_2
S_2
310b
308b
306b
BS
Waveguide with focusing lens
Plasmonic antenna
Sub-diffraction spot
Femtosecond Laser, linearly polarized pulses
300
302
304

FIG. 13

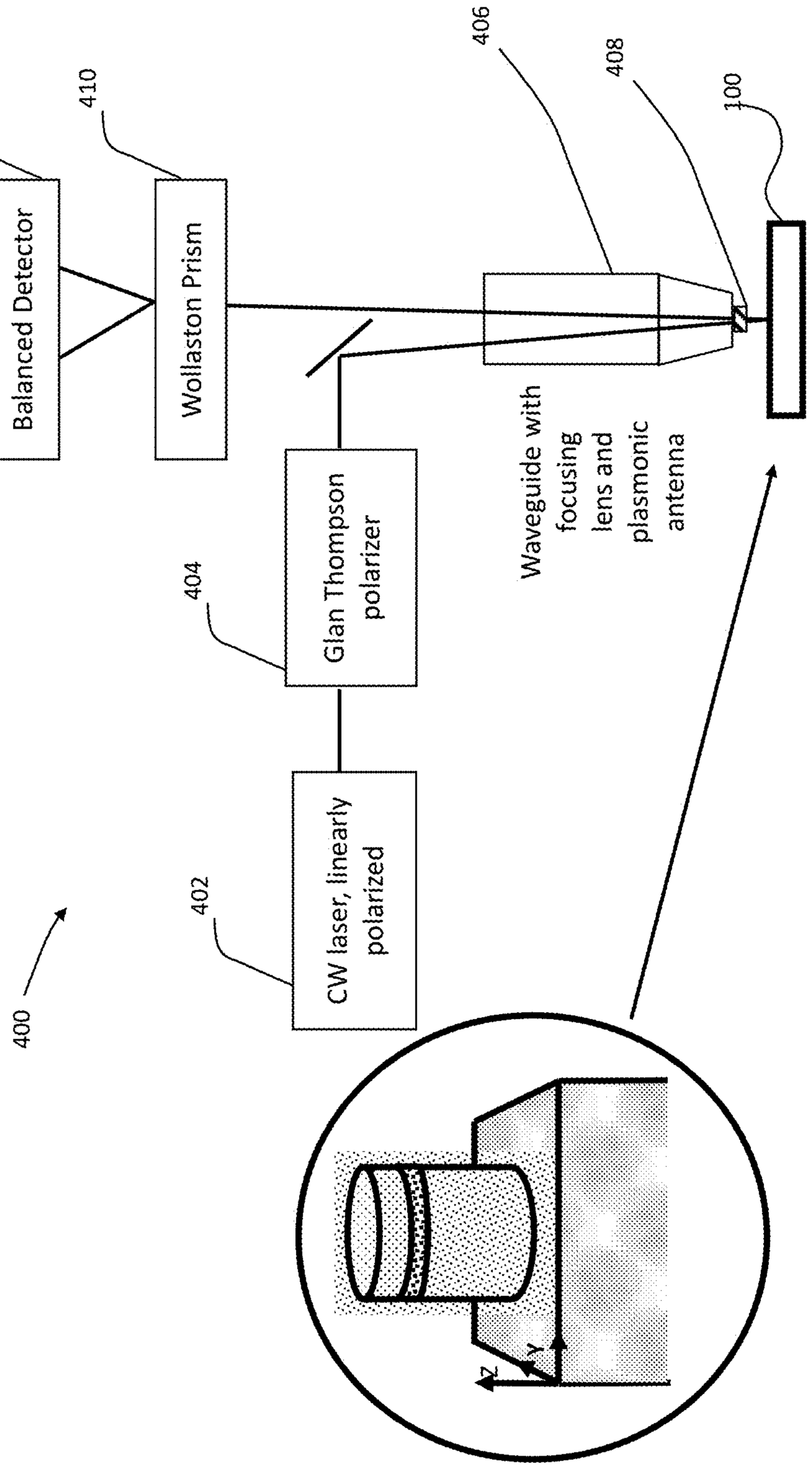
400
402
CW laser, linearly polarized
404
Glan Thompson polarizer
406
Waveguide with focusing lens and plasmonic antenna
408
100
Sample
410
Wollaston Prism
412
Balanced Detector
z
y

FIG. 14

ALL-OPTICAL WRITE/READ SCHEME FOR MAGNETIC NANOSTRUCTURES

CROSS-REFERENCE TO RELATED APPLICATIONS

The present patent application is related to and claims the priority benefit of U.S. Non-Provisional patent application Ser. No. 16/399,917 filed Apr. 30, 2019 titled "SURFACE-PLASMON OPTO-MAGNETIC FIELD ENHANCEMENT FOR ALL-OPTICAL MAGNETIZATION SWITCHING" now U.S. Pat. No. 10,739,261 to Dutta et al., and U.S. Provisional Patent Application Ser. No. 62/664,925 filed Apr. 30, 2018, titled "Surface-plasmon opto-magnetic field enhancement for all-optical magnetization switching" the contents of each of which are hereby incorporated by reference in their entirety into the present disclosure.

STATEMENT REGARDING GOVERNMENT FUNDING

This invention was made with government support under N00014-16-1-3003 awarded by the Office of Naval Research. The government has certain rights in the invention.

TECHNICAL FIELD

The present disclosure generally relates to optomagnetic devices, and in particular, to optomagnetic devices with nanostructures.

BACKGROUND

This section introduces aspects that may help facilitate a better understanding of the disclosure. Accordingly, these statements are to be read in this light and are not to be understood as admissions about what is or is not prior art.

The demand for faster devices operating in ps or fs regimes is now here corresponding with Moore's law. Consequently, at these speeds the need for lower energy devices is critical. Thus, spintronics is now becoming a choice technology for a variety of different applications including memory and logic. The magnetic tunnel junction is now the most ubiquitous spintronic memory device in which the magnetization of the storage layer is switched by spin-transfer-torque or spin-orbit torque interactions. Whereas these novel spin-torque interactions exemplify the potential of electron-spin-based devices and memory, the switching speed is limited to the ns regime because of the precessional motion of the magnetization. In particular, state of the art spin-transfer-torque magnetic tunnel junctions (STT-MTJ) require high current densities of the order of 10^7-10^8 A/cm^2, making them unattractive from an energy consumption perspective for high frequency applications of ps or fs magnetization switching. In addition such high current densities can result in electrical breakdown of the MgO tunnel barrier, negatively impacting their reliability.

An all-optical magnetization switching, largely based on the inverse Faraday effect, has been shown to be an attractive method for achieving magnetization switching at ps speeds. While these devices have been shown to operate at the desired switching speeds, they are not compatible with semiconductor manufacturing processing.

Therefore, there is an unmet need for a novel optical switching mechanism that can work with semiconductor-based ultra-high density integrated nanostructure fabrication.

SUMMARY

A system of writing to and reading from a magnetic nanostructure is disclosed. The system includes an opto-magnetic write arrangement. The arrangement includes a polarizer configured to receive incident light and provide a circularly or linearly polarized light. Light polarization is controlled by the polarizer and its orientation with respect to polarization of the incident light. The system also includes a nanomagnetic structure configured to receive the polarized light. The nanomagnetic structure a substrate, and a nano-magnetic stack. The nanomagnetic stack includes a nano-magnet, and a capping layer. The nanomagnetic stack is configured to receive the polarized light and thereby switch orientation of a magnetic moment associated with the magnetic nanostructure whereby the magnetic moment direction specifies a bit value held in the magnetic structure. The system further includes a magnetic read arrangement, configured to receive and interpret an optical signal from the magnetic nanostructure indicating the magnetic moment orientation from the nanomagnetic stack.

BRIEF DESCRIPTION OF DRAWINGS

FIG. **1** is a schematic diagram of a coupled magneto-plasmonic nanostructure with a magneto-plasmonic stack including a nano-sized plasmonic resonator coupled to a nanomagnet, according to the present disclosure.

FIG. **2** is a schematic diagram of a coupled nanomagnetic structure including a substrate and a nanomagnet but without the nanosized plasmonic resonator provided for comparison to the magneto-plasmonic structure shown in FIG. **1**.

FIG. **3** is a graph of permittivity (real part, ε', on the left and imaginary part, ε", on the right: $\hat{\varepsilon}=\varepsilon'(\omega)+\varepsilon''(\omega)$) for Bi-substituted iron garnet (BIG) used as the material for the nanomagnet of FIG. **1**.

FIG. **4** is a graph of permittivity (real part, ε", on the left and imaginary part, ε", on the right: $\hat{\varepsilon}=\varepsilon'(\omega)+\varepsilon''(\omega)$) for Gadolinium Iron Cobalt (GdFeCo) used as the material for the nanomagnet of FIG. **1**.

FIG. **5** is a graph of permittivity (real part, ε', on the left and imaginary part, ε", on the right: $\hat{\varepsilon}=\varepsilon'(\omega)+\varepsilon''(\omega)$) for Titanium Nitride (TiN) used as the material for the nano-sized plasmonic resonator of FIG. **1**.

FIG. **6***a* is the z-component of the opto-magnetic field intensity in units of Tesla (T) vs. length in nm along the diameter of BIG-TiN interface in the x-axis for a 10 nm thick BIG layer in the magneto-plasmonic structure of FIG. **1** vs. the nanomagnetic structure of FIG. **2**.

FIG. **6***b* is a graph showing dependence of the z-component of the opto-magnetic field in T vs wavelength in nm for the magneto-plasmonic structure of FIG. **1** at the center of the magneto-plasmonic stack at the interface of the nano-sized plasmonic resonator and the nanomagnet.

FIG. **7***a* is a graph of electric field components along the x-axis of the of the nano-sized plasmonic resonator and the nanomagnet interface of the magneto-plasmonic stack of FIG. **1**.

FIG. **7***b* is an output of the electric field intensity showing a near-field enhancement for the magneto-plasmonic structure of FIG. **1** about the interface of the nano-sized plas-

monic resonator and the nanomagnet with BIG as the choice for the nanomagnet in the xy plane.

FIG. **7***c* is a graph of the electric field components along the x-axis of the nanomagnet-substrate interface for the nanomagnetic structure shown in FIG. **2** with BIG as the choice for the nanomagnet.

FIG. **7***d* is an output of the electric field intensity showing the nonmagnetic structure of FIG. **2** about the interface of the substrate and the nanomagnet with BIG as the choice for the nanomagnet in the xy plane.

FIG. **8***a* is a graph of the z-component of opto-magnetic field H_{OM} obtained for the magneto-plasmonic structure of FIG. **1** and the nanomagnetic structure of FIG. **2** with illumination of circularly polarized light at 710 nm wavelength with a 10 nm thick GdFeCo nanomagnet.

FIG. **8***b* is an output of the electric field intensity showing a near-field enhancement for the magneto-plasmonic structure of FIG. **1** about the interface of the nano-sized plasmonic resonator and the nanomagnet with GdFeCo as the choice for the nanomagnet in the xy plane.

FIG. **8***c* is a graph of the electric field components along the x-axis of the nanomagnet-substrate interface for the nanomagnetic structure shown in FIG. **2** with GdFeCo as the choice for the nanomagnet in the xy plane.

FIG. **9** is a graph of the opto-magnetic field z-component along the x-axis in the xy plane of the interface of the nano-sized plasmonic resonator and the nanomagnet for the structure of the magneto-plasmonic structure of FIG. **1** (BIG-TiN) with 20 nm diameter.

FIG. **10** is a graph of the electric field intensity plot along the diameter in the x-axis plane of the interface of the nano-sized plasmonic resonator and the nanomagnet for the structure of the magneto-plasmonic structure of FIG. **1** (BIG-TiN) shown for a 20 nm diameter.

FIG. **11***a* is an electric field intensity output along the x-axis of the interface of the nano-sized plasmonic resonator and the nanomagnet for the structure of the magneto-plasmonic structure of FIG. **1** (BIG-TiN) shown for a 20 nm diameter.

FIG. **11***b* is an electric field intensity output along the yz plane of the magneto-plasmonic stack of FIG. **1** (TiN-BIG) perpendicular to the interface of the nano-plasmonic resonator and the nanomagnet shown for a 20 nm diameter.

FIG. **12** is a graph of $\delta H_{OM,z}/\delta\lambda$ measured in T/nm as well as $H_{OH,z}$ in T vs. wavelength in nm for the magneto-plasmonic structure of FIG. **1**, showing a maximum magnitude of $\delta H_{OM,z}/\delta\lambda$ T/nm at a wavelength of about 730 nm.

FIG. **13** is a schematic of a write circuit, employing the magneto-plasmonic structure of FIG. **1**.

FIG. **14** is a schematic of read circuit, employing the magneto-plasmonic structure of FIG. **1**.

DETAILED DESCRIPTION

For the purposes of promoting an understanding of the principles of the present disclosure, reference will now be made to the embodiments illustrated in the drawings, and specific language will be used to describe the same. It will nevertheless be understood that no limitation of the scope of this disclosure is thereby intended.

In the present disclosure, the term "about" can allow for a degree of variability in a value or range, for example, within 10%, within 5%, or within 1% of a stated value or of a stated limit of a range.

In the present disclosure, the term "substantially" can allow for a degree of variability in a value or range, for example, within 90%, within 95%, or within 99% of a stated value or of a stated limit of a range.

Optical-only magnetization switching has been shown in recent years to overcome the aforementioned ns regime precession dynamics limits. Thus, 40-fs circularly polarized laser pulses have been employed to reversibly switch the magnetization by changing the light helicity in a wide range of magnetic materials. Circularly polarized laser pulses provide an effective magnetic field via the inverse Faraday effect. This opto-magnetic field is proportional to $[E(\omega)\times E^*(\omega)]$ where (E is the light electric field). This opto-magnetic field, H_{OM}, is largely responsible for the ultrafast magnetization reversal. The magnitude of this field depends on the intensity of the incident light as given by the following equation:

$$H_{OM}=\beta\varepsilon_0(E(\omega)\times E^*(\omega)) \tag{1}$$

where β is the magneto-optical susceptibility of the magnetic material,

ε_0 is the permittivity of free space, and

E is the magnitude of electric-field of the electromagnetic wave inside the magnetic material.

The magneto-optical susceptibility is calculated using the following equation:

$$\beta = \frac{\theta_F \lambda n}{A = \pi d M_0} \tag{2}$$

where θ_F is the Faraday rotation at wavelength λ for a magnetic material layer with magnetization M_0 and real part of refractive index n. Using the above relationships, in the present disclosure, the effect on the opto-magnetic field of surface plasmons generated with circularly polarized light at the interface between magnetic materials and plasmon resonators is used to generate a novel on-chip integration of nanoscale photonic and magnetic devices. The magnitude of the plasmon-generated opto-magnetic field, H_{OM}, is enhanced by about 10 times in comparison to that resulting from the direct photon-magnetic material coupling. In particular, this enhancement is observed when the magnetic material is behaves as a dielectric rather than metallic at optical frequencies rather than a conventional metallic thin film.

Plasmonics is a phenomenon utilized in the novel structure of the present disclosure. Plasmonics deals with the study of the oscillations of free electrons in a metal coupled to an electromagnetic field. In particular Surface plasmon polaritons (SPPs) are infrared or visible-frequency electromagnetic waves that travel along a metal-dielectric or metal-air interface. They are a type of surface wave, guided along the interface in much the same way that light can be guided by an optical fiber. SPPs are shorter in wavelength than the incident light. Hence, SPPs can have tighter spatial confinement and higher local field intensity. Therefore, plasmonics enables the localization of electromagnetic energy to dimensions much smaller than the diffraction limit of light. This phenomenon was advantageously utilized to generate plasmonic resonators coupled to nanomagnet structures to provide the novel structure of the present disclosure. As a result opto-magnetic fields are generated under illumination with circularly polarized light. In particular, under identical laser fluences, significantly larger opto-magnetic fields are generated in the coupled plasmonic/magnetic nanostructures when compared to direct light excitation of the nanomagnet. Therefore, with the larger opto-magnetic fields obtained for

the same input intensity of light being acted upon the nano-magnets the high desired switching can be realized with all the benefits of high efficiency, low-energy opto-magnetic switching of the prior art which could not have been implemented in nano-structures. Earlier, magnetic tunnel junctions (referred to above) used magnetic materials with in-plane magnetic anisotropy. However, it has been shown that layers with perpendicular magnetic anisotropy can lower the necessary write current density. In the present disclosure, perpendicular magnetic anisotropy (PMA) and the associated magnetic materials and structures are used in the switching of nanomagnets. Therefore, discussion in the present disclosure pertains mainly to the z-component of the opto-magnetic field generated by surface plasmons. However, the teachings of the present disclosure are readily applicable to in-plane magnets. Additionally, it should be appreciated that these teachings also apply to switching magnets engineered to exhibit tilted magnetization orientation.

Referring to FIG. **1** a schematic diagram of a coupled magneto-plasmonic structure **100**, according to the present disclosure, is provided. The magneto-plasmonic structure **100** includes a substrate **102** (shown in a cubical form for demonstration purposes, however, the substrate **102** can be in any form appropriate for the implementation of the magneto-plasmonic structure **100** in a high-speed switching system). The substrate is an optically transparent dielectric layer, e.g., magnesium oxide, sapphire, or other suitable dielectrics known to a person having ordinary skill in the art. The magneto-plasmonic structure **100** also includes a magneto-plasmonic stack **103** comprising a plasmonic resonator **104**, a nanomagnet **106**, and a capping layer **108**. In FIG. **1**, light **110** is shone from below. The circular arrow **112** depicts illumination which is circularly polarized light and the curly arrow **114** indicates the direction of incidence of the light **110**. Circularly polarized light, as known to a person having ordinary skill in the art, refers to an electromagnetic wave in which, at each point, the electric field of the wave has a constant magnitude but its direction rotates with time at a steady rate in a plane perpendicular to the direction of the wave. light with orthogonal electric field components phase shifted by 90°. Such electric fields of electromagnetic waves can be produced from linearly polarized light using a circular polarization filter such as a zero-order quarter waveplate or any other component known to a person of skill in this art that produces circular from linearly polarized electromagnetic fields. To enable compatibility with high-speed complementary metal oxide semiconductor (CMOS) needs, low-loss CMOS compatible refractory metals are utilized instead of gold and silver, i.e., metals which are known to exhibit strong plasmonic activity but are CMOS-incompatible. In this regard, refractory transition metal nitrides have emerged as suitable candidates for the visible and near-infrared (NIR) plasmonic applications. In particular, titanium nitride exhibits optical properties comparable to those of gold, it is compatible with current nanofabrication technologies and can be epitaxially grown on c-sapphire and magnesium oxide (MgO) which all make good substrate choices for the structures of the present disclosure. Therefore, an exemplary choice of material for the plasmonic resonator **104** is titanium nitride (TiN) with the substrate **102** made of MgO. For the thin nanomagnet **106**, exemplary choices for the magnetic PMA materials include Bi-substituted iron garnet (BIG) and Gadolinium Iron Cobalt (GdFeCo), however, other nanomagnets, known to a person having ordinary skill in the art can also be used.

For the capping layer **108** Si_3N_4 was used as an exemplary material. The following dimensional ranges are provided for the magneto-plasmonic structure **100**, according to the present disclosure, however, it should be understood that other dimensions can be used for specific application, and therefore no limitation is intended by the use of these dimensions. The magneto-plasmonic stack **103** has a diameter between about 10 nm and about 100 nm with the plasmonic resonator **104** having a thickness of about 10 nm to about 50 nm and the capping layer **108** having a thickness of about 10 nm to about 40 nm. The thickness of the nanomagnet **106** was held at about 10 nm for both types of magnetic materials, BIG and GdFeCo. The effect of increasing/decreasing the diameter of the magneto-plasmonic stack **103** on the magnitude of the opto-magnetic field H_{OM} is further described below. Plasmonic resonances (wavelength, intensity) in these stacks depend on the intrinsic optical properties of the constituent materials and their dimensions. For example for the case of TiN and the magneto-plasmonic stack **103** having a diameter of about 30 nm, it exhibits strong plasmonic activity in the visible and NIR. The choice of Si_3N_4 as the material for the capping layer **108** and its thickness (about 10 nm to about 40 nm) allows plasmonic excitations in the visible/NIR wavelength region of interest. Normal incidence illumination by circularly polarized light through the substrate **102** is arranged, as shown in FIG. **1** and denoted by the circular arrow **112** and the curly arrow **114**. While the incident light is shone from below and through the substrate **102**, it should be appreciated that incidence from above the substrate would also provide similar results to those outlined in the present disclosure. The excitation wavelength is chosen to match the TiN nanodisk plasmonic resonance. This is determined to be about 710 nm for the material dimensions and optical constants employed, however, other wavelengths would be appropriate for other material selection and dimensions. The illumination intensity is chosen as about 1 mJ/cm^2.

Referring to FIG. **2**, a schematic diagram of a coupled nanomagnetic structure **200** is also provided, for comparison to the magneto-plasmonic structure **100** shown in FIG. **1**. Similarly, the nanomagnetic structure **200** includes a substrate **202**. The substrate is an optically transparent dielectric layer, e.g., magnesium oxide or other suitable dielectrics known to a person having ordinary skill in the art. The nanomagnetic structure **200** also includes a non-plasmonic stack **203** (as compared to the magneto-plasmonic stack **103**) comprising a nanomagnet **206**, and a capping layer **208**. In FIG. **2**, light **210** is shone from below. The circular arrow **212** depicts illumination which is circularly polarized light and the curly arrow **214** indicates the direction of incidence of the light **210**.

As will be discussed below, almost an order of magnitude increase in the magnitude of the opto-magnetic field when the interaction with the nanomagnet is via the magneto-plasmonic stack **103** and in particular with the plasmonic resonator **104** (see FIG. **1**) as compared to the non-plasmonic stack **203** (see FIG. **2**). This significant increment is attributed to the near-field enhancement induced by the plasmonic resonator **104** (see FIG. **1**) exhibiting surface plasmon resonances (LSPR), as is known to a person having ordinary skill in the art. This enhancement indicates efficient coupling of electromagnetic radiation with the magneto-plasmonic structure **100** as compared to direct illumination of nanomagnets as it is done in experiments reported thus far on optical-only magnetization switching.

Referring back to FIGS. **1** and **2**, the material of the thin nanomagnets **106** and **206**, were exemplarily provided as

BIG and GdFeCo. Referring to FIGS. **3** and **4**, graphs of permittivity (real part, ε', on the left and imaginary part, ε", on the right: $\hat{\varepsilon}=\varepsilon'(\omega)+\varepsilon''(\omega)$) are provided for BIG and GdFeCo which show the optical properties of BIG and GdFeCo in the visible and near-infrared regions. Referring to FIG. **5**, graphs of permittivity (real part, ε', on the left and imaginary part, ε", on the right: $\hat{\varepsilon}=\varepsilon'(\omega)+\varepsilon''(\omega)$) are provided for TiN which show the optical properties of plasmonic TiN derived from spectroscopic ellipsometry measurements of sputter-deposited 30 nm thick TiN thin films on MgO. Comparison of FIGS. **4** and **5** indicate that at 710 nm, BIG behaves as a lossless dielectric (ε" is zero) whereas GdFeCo is a lossy metal. This results in plasmonic resonances in the magneto-plasmonic structure **100** (see FIG. **1**) sample at the plasmonic resonator **104**-nanomagnet **106** interface when the material choice is TiN-BIG, in contrast to when the material choice is TiN—GdFeCo. While both GdFeCo and TiN are metallic in nature, the former being a relatively weaker metal (lower value of negative ε'). In this case we observe weak plasmonic resonances at the nanomagnet **106** and capping layer **108** interface (i.e., the GdFeCo—Si_3N_4 interface).

In order to understand the plasmonic resonance, illumination of individual BIG-TiN interface in the magneto-plasmonic structure **100** (see FIG. **1**) and the nanomagnet **206** in the non-plasmonic stack **203** (see FIG. **2**) were considered separately and the electric field distribution characteristic of the plasmon resonance at 710 nm wavelength were studied. Utilizing Eq. (1), the opto-magnetic field H_{OM} was derived. The magnetic susceptibility β is calculated using Eq. (2) with experimentally reported values θ_F and M_0 for BIG. Referring to FIG. **6***a*, a comparison of the z-component of the opto-magnetic field intensity in T vs. length in nm across the 50 nm diameter of BIG-TiN interface in the x-axis in the magneto-plasmonic structure **100** (see FIG. **1**, in FIG. **6***a* nanomagnet with TiN resonator, upper panel) and the nanomagnetic structure **200** (see FIG. **2**, in FIG. **6***a* only nanomagnet, lower panel) is provided. Illumination is with circularly polarized light of intensity 1 mJ/cm^2 at 710 nm wavelength under normal incidence. Note, the plasmonic resonator **104** and the capping layer **108** thicknesses are about 30 nm and about 20 nm respectively. Referring to FIG. **6***b* a graph of wavelength in nm dependence of the z-component of the opto-magnetic field in T for the magneto-plasmonic structure **100** (see FIG. **1**) sample (about 50 nm diameter) at the stack center at the TiN-BIG interface is also provided. It can be clearly seen a 10-fold enhancement in the z-component of the opto-magnetic field in the magneto-plasmonic structure **100** (see FIG. **1**) sample compared to the non-plasmonic stack **203** (see FIG. **2**) sample. In particular, the parameter $H_{OM,Z}$ has a value of about 5.98T for the magneto-plasmonic structure **100** (see FIG. **1**) using TiN-BIG vs. about 0.589T for the nanomagnetic structure **200** and its non-plasmonic stack **203** (see FIG. **2**) using MgO-BIG. The enhancement in $H_{OM,Z}$ due to the plasmon resonance at 710 nm wavelength is also apparent (see FIG. **6***b*).

Detailed electromagnetic analysis of the BIG in the magneto-plasmonic structure **100** (see FIG. **1**) and the nanomagnetic structure **200** when illuminated with circularly polarized light at 710 nm is provided below. When a plasmonic nanodisk is illuminated with circularly polarized light it generates a rotating dipole moment that is associated with the plasmonic resonance. Referring to FIGS. **7***a* and **7***c* electric field components along the x-axis of the BIG-TiN interface for the magneto-plasmonic structure **100** (see FIG. **1**), shown in FIG. **7***a*, and the BIG-MgO interface for the nanomagnetic structure **200** (see FIG. **2**), shown in FIG. **7***c* are shown, respectively. Correspondingly, near-field enhancement for the magneto-plasmonic structure **100** (see FIG. **1**), shown in FIG. **7***b*, as compared to the BIG-MgO interface as well as a vertical cross-section of the entire stack (yz plane) for the nanomagnetic structure **200** (see FIG. **2**), shown in FIG. **7***d* are provided where such enhancement is due to the plasmon resonance. Such a field enhancement is responsible for the increase in the opto-magnetic field of the magneto-plasmonic structure **100** (see FIG. **1**), as discussed above. A noticeable feature of the plasmon resonance is that it introduces an out-of-plane component of the electric field E_z whereas the incident light has no such z-component. This out-of-plane component of the electric field E_z is a well-known feature of the plasmon resonance. For calculating the opto-magnetic field we have used only the out-of-plane component of the magnetic susceptibility β. Thus, the opto-magnetic field reported in the figures, corresponds only to the z-component of H_{OM}. It should be appreciated that due to the presence of additional components of the electric field, plasmon resonances can in principle generate in-plane components of the opto-magnetic field $H_{OM,x/y}$. The amplitudes of these components depend on the magnitude of β in the x,y plane. Such an in-plane component of H_{OM} can lead to more efficient switching of magnets with canted magnetization orientation.

Referring to FIG. **8***a*, the results of the opto-magnetic field H_{OM} obtained for the magneto-plasmonic structure **100** (see FIG. **1**) and the nanomagnetic structure **200** (see FIG. **2**) samples under illumination of circularly polarized light at 710 nm wavelength are shown when the BIG has been replaced with a 10 nm thick GdFeCo nanomagnet. The magnetic susceptibility is $1.7*10^{-6}$ m/A. As discussed with reference to FIG. **4** above, GdFeCo is metallic in the visible/near-infrared region of the electromagnetic spectrum. Therefore in this case no plasmonic field enhancement at the GdFeCo—TiN interface is observed as both layers are metallic. In contrast, a plasmonic near-field enhancement at the GdFeCo—Si_3N_4 interface is observed in the magneto-plasmonic structure **100** (see FIG. **1**) sample, although this enhancement is weaker. This enhancement is clearly shown in FIGS. **8***b* and **8***c* where the electric field intensity for the GdFeCo of the magneto-plasmonic structure **100** (see FIG. **1**) sample and the nanomagnetic structure **200** (see FIG. **2**) sample are provided, respectively. The reason for the weaker field enhancement is because compared to TiN at 710 nm wavelength, GdFeCo is a more lossy (higher ε") and weaker (lower negative ε') metal. The plasmonic resonance is mostly dominated by GdFeCo, with the TiN contribution to the plasmon resonance being significantly reduced. Hence the magneto-plasmonic structure **100** (see FIG. **1**) with GdFeCo does not exhibit large opto-magnetic field enhancement compared to the nonmagnetic structure **200** (see FIG. **2**). We note an opto-magnetic field enhancement of only 3.4 in the magneto-plasmonic structure **100** (see FIG. **1**) sample compared to the nanomagnetic structure **200** (see FIG. **2**) sample which is less than what we observed for BIG due to aforementioned reasons. Although GdFeCo exhibits PMA for thicknesses >10 nm, the use of thicker layers would result in reduction of the contributions of the TiN plasmonic resonator on the opto-magnetic field enhancement. It can be clearly seen a 3-fold enhancement in the z-component of the opto-magnetic field in the magneto-plasmonic structure **100** (see FIG. **1**) sample compared to the non-plasmonic stack **203** (see FIG. **2**) sample. In particular, the parameter $H_{OM,Z}$ has a value of about 0.75T for the magneto-plasmonic structure **100** (see FIG. **1**) using TiN—GdFeCo vs. about 0.22T for the nanomagnetic structure **200** and its non-plasmonic stack **203** (see FIG. **2**) using MgO—GdFeCo.

Next, the dependence of the opto-magnetic field enhancement on the diameter of the magneto-plasmonic stack **103** (see FIG. **1**) is discussed. It is well-known that plasmonic resonances in metal nanodisks strongly depend on their size. A change in size can alter the strength of the plasmon resonance. FIG. **9** is a graph of the opto-magnetic field z-component along the x-axis in the xy plane of the BIG-TiN interface for the structure of the magneto-plasmonic structure **100** (see FIG. **1**) with 20 nm diameter. A clear enhancement in $H_{OM,Z}$ of about The enhancement in $H_{OM,Z}$ due to the plasmon resonance at 710 nm wavelength is also apparent (see FIG. **6***b*). However, a comparison of FIG. **6***a* and FIG. **9** indicate that a reduction of the stack diameter of the magneto-plasmonic structure **100** (see FIG. **1**) sample reduces the plasmonic enhancement in H_{OM} from about 10-fold to about 4-fold. Also the nature of the opto-magnetic field along the diameter is different. This difference is due to the weaker nature of the plasmon resonance for the sample with reduced diameter. Referring to FIG. **10** a graph of electric field intensity plot along the yz plane of the magneto-plasmonic stack **103** (see FIG. **1**) is shown for a 20 nm diameter. Illumination is with circularly polarized light of intensity 1 mJ/cm^2 at 710 nm wavelength. Comparing FIGS. **7***a* and **10**, one can clearly see that the y-component of the electric field is reduced upon reducing the diameter. FIG. **7***a* corresponds to a 50 nm diameter stack whereas FIG. **10** is for the 20 nm stack. This leads to a reduction in $H_{OM,Z}$. Also the variation of the y-component of the electric field of light along the stack diameter is slightly different upon reducing the diameter of the stack. Consequently there is a change in the way $H_{OM,Z}$ varies along the diameter when the stack diameter is reduced. Nevertheless, the plasmonic enhancement in $H_{OM,Z}$ still persists. This illustrates that plasmon mediated magnetic switching is compatible with dimensionality reduction of nanomagnets for ultra-high density storage and it points to opportunities to increase the effect by matching the excitation light source to the plasmon resonance. Referring to FIGS. **11***a* and **11***b*, electric field components along the x-axis of the TiN-BIG interface and electric field intensity plot along the yz plane of the magneto-plasmonic stack **103** with 20 nm diameter (see FIG. **1**) are shown, respectively. Again, illumination is with circularly polarized light of intensity 1 mJ/cm^2 at 710 nm wavelength.

It should be appreciated that the optical anisotropy of both GdFeCo and BIG magnetic layers were ignored. This is because the off-diagonal terms of the permittivity tensor for both materials, obtained from the product of β and M_0 are at least an order of magnitude lower than the diagonal terms as shown in FIGS. **3** and **4**.

TABLE 1

Summary of Results

Magnetic Material	n	θ_F (deg.)	M_0 (A/m)	β (m/A)	FOM
BIG	2.9	0.027 [25]	$5.5 * 10^4$ [26]	$5.7 * 10^{-7}$	10
GdFeCo	3.45	0.75 [5]	$1 * 10^5$ [5]	$1.7 * 10^{-6}$ [5]	3.4

where figure of merit (FOM) is calculated from

$$H_{OM} = \frac{H_{OM,z(Plasmonic\ Stack)}}{H_{OM,z(non\text{-}plasmonic\ stack)}} \quad (3)$$

where the plasmonic stack is shown in FIG. **1** and non-plasmonic stack is shown in FIG. **2**.

Referring to FIG. **12**, graph of $\delta H_{OM,z}/\delta\lambda$ measured in T/nm as well as $H_{OM,z}$ in T vs. wavelength in nm is provided for the magneto-plasmonic structure **103** of FIG. **1**, showing a maximum $\delta H_{OH,z}/\delta\lambda$ T/nm at a wavelength of about 700 nm with BIG for nanomagnet **106**. This is a parameter that can be used to distinguish the structure of the present disclosure from those of the prior art.

These results show that surface plasmon resonances can lead to significant near-field enhancement and thereby much higher opto-magnetic field H_{OM} compared to free space excitation. In particular, the present disclosure sets out a showing that the magnitude of the plasmon-generated opto-magnetic field, H_{OM}, is enhanced in comparison to that resulting from the direct photon-magnetic material coupling to the tune of about 10 time the magnetic material that behaves as a dielectric at optical frequencies is coupled to a plasmonic resonator. The present disclosure also provides that the optical properties of the magnetic material play an important role in determining the strength of the plasmon resonance and hence an optimal choice of material is necessary in order to achieve the highest possible H_{OM}. The present disclosure also provides a roadmap of having in-plane components of the opto-magnetic field H_{OM} associated with surface plasmon resonances. Thus, the proposed approach could potentially enable future on-chip plasmonic-magnetic devices for photonics, spintronics and hybrid devices.

Referring to FIG. **13**, a schematic of a write circuit **300**, employing the magneto-plasmonic structure of FIG. **1**, is provided. The write circuit **300** is driven by a femtosecond laser **302**. The output of the laser passes through a beam splitter **304** (identified in the schematic as BS) which divides the laser output into two beams of equal power. Each split beam line has a polarizer **306***a* or **306***b* (identified in the schematic as P**1** or P**2**) to further improve the degree of linear the beam polarization followed by a zero order air-gap quarter waveplate **308***a* or **308***b* (identified in the schematic as QW**1** or QW**2**) and controlled by an electrically or optically controlled switch **310***a* or **310***b* (identified in the schematic as S**1** or S**2**) that allows the user to select one or more laser pulses to be fed to a beam coupler **312**. The zero order air-gap quarter waveplates **308***a* and **308***b* (identified in the schematic as QW**1** and QW**2**) are configured to provide orthogonal circular polarizations (left or right) at their respective output. The output of the electrically or optically controlled switches **310***a* and **310***b* (identified in the schematic as S**1** and S**2**) are fed into the polarization maintaining beam coupler **312**. At any instant, at the output of the beam coupler **312**, either of the pulse(s) through the electrically or optically controlled switches **310***a* or **310***b* (identified in the schematic as S**1** or S**2**), whichever is on, will be present. These pulse(s) is(are) fed to a waveguide **314** with a plasmonic antenna **316** at a distal end to generate a sub-diffraction beam spot **318** to write on the magneto-plasmonic stack **103** (see FIG. **1**).

Referring to FIG. **14**, a read circuit **400** is shown. In this example, the read circuit **400** is driven by a continuous wave laser with linear polarization **402**. It is understood by those skilled in the art that the read laser can also be a pulsed laser, and referring to the write circuit **300**, the pulsed laser can be derived from the same fs laser of **302**. A Glan-Thompson polarizer **404** further improves the degree of linear polarization of the incident beam. The output then passes through a similar waveguide **406** setup as in the read circuit **400** with lens and plasmonic antenna **408** to achieve sub-diffraction spot size (not shown). The reflected beam is again captured by the same waveguide and fed into a Wollaston prism **410**

which splits the beam into two orthogonal components. These components are fed into a balanced photodetector **412** which provides an electrical output proportional to the difference in the intensities of the two orthogonal components. A positive/negative output corresponds to up/down (or down/up) orientation of the magnet in the magneto-plasmonic stack **103** (see FIG. **1**).

The write circuit **300** performs the write operation as follows: Depending on the hellicity of the circularly polarized light (i.e., clockwise or counter-clockwise), the magnetization is switched from downward to upward. In particular, when one of the electrically or optically controlled switches **310***a* or **310***b* (identified in the schematic as S**1** or S**2**) is activated to allow left or right circular pulses which when incident upon the magneto-plasmonic structure **100** (see FIG. **1**) would toggle the magnetization. For example, if the electrically or optically controlled switch **310***a* (identified in the schematic as S**1**) is opened and the electrically or optically controlled switch **310***b* (identified in the schematic as S**2**) is closed, right circularly polarized light is incident on the sample and the magnetization at the magneto-plasmonic structure **100** (see FIG. **1**) would be downward. To reverse the magnetization (or bit), if the electrically or optically controlled switch **310***a* (identified in the schematic as S**1**) is closed and the electrically or optically controlled switch **310***b* (identified in the schematic as S**2**) is opened to allow left circularly polarized pulses, then the magnetization at the magneto-plasmonic structure **100** (see FIG. **1**) would be upward.

While, the write circuit **300** and the read circuit **400** are shown in specific implementations, other implementations are also possible. One key factor is to generate the needed circular polarizations to establish the rotational direction and thereby establish the bit within the structure of FIG. **1**.

Those having ordinary skill in the art will recognize that numerous modifications can be made to the specific implementations described above. The implementations should not be limited to the particular limitations described. Other implementations may be possible.

The invention claimed is:

1. A system of writing to and reading from a magnetic nanostructure, comprising:

an opto-magnetic write arrangement, comprising:

a polarizer configured to receive incident light and provide a circularly or linearly polarized light, wherein light polarization is controlled by the polarizer and its orientation with respect to polarization of the incident light;

a nanomagnetic structure configured to receive the polarized light, the magnetic nanostructure comprising:

a substrate, and

a nanomagnetic stack, comprising:

a nanomagnet, and

a capping layer,

wherein the nanomagnetic stack is configured to receive the polarized light and thereby switch orientation of a magnetic moment associated with the magnetic nanostructure

whereby the magnetic moment direction specifies a bit value held in the magnetic structure; and

a magnetic read arrangement, configured to receive and interpret an optical signal from the magnetic nanostructure indicating the magnetic moment orientation from the nanomagnetic stack.

2. The system of claim **1**, wherein the substrate is made of an optically transparent material dielectric.

3. The system of claim **2**, wherein the optically transparent material is selected from the group consisting essentially of MgO and c-sapphire.

4. The system of claim **1**, wherein the nanomagnet is one of a ferromagnet, a ferrimagnet or an antiferromagnet having magnetic perpendicular anisotropy.

5. The system of claim **4**, wherein the nanomagnet selected from the group consisting essentially of Bi-substituted iron garnet (BIG) and Gadolinium Iron Cobalt (GdFeCo).

6. The system of claim **1**, wherein the capping layer is Si_3N_4.

7. The system of claim **1**, wherein diameter of the magnetic stack is between about 10 nm and 20 nm.

8. The system of claim **1**, wherein the wavelength of the polarized light is between 660 nm and 740 nm.

* * * * *